



Texas Water Journal

Volume 11 Number 1 | 2020





Texas Water Journal

Volume 11, Number 1

2020

ISSN 2160-5319

texaswaterjournal.org

THE TEXAS WATER JOURNAL is an online, peer-reviewed journal devoted to the timely consideration of Texas water resources management, research, and policy issues. The journal provides in-depth analysis of Texas water resources management and policies from a multidisciplinary perspective that integrates science, engineering, law, planning, and other disciplines. It also provides updates on key state legislation and policy changes by Texas administrative agencies.

For more information on TWJ as well as TWJ policies and submission guidelines, please visit texaswaterjournal.org.

Editorial Board

Todd H. Votteler, Ph.D.

Editor-in-Chief

Collaborative Water Resolution LLC

Kathy A. Alexander, Ph.D.

Gabriel Collins, J.D.

Center for Energy Studies

Baker Institute for Public Policy

Robert E. Mace, Ph.D.

Meadows Center for Water and the Environment

Texas State University

Ken A. Rainwater, Ph.D.

Texas Tech University

Rosario Sanchez, Ph.D.

Texas Water Resources Institute

Jude A. Benavides, Ph.D.

University of Texas, Rio Grande Valley

Managing Editor

Chantal Cough-Schulze

Texas Water Resources Institute

Layout Editor

Sarah Richardson

Texas Water Resources Institute

Staff Editor

Kristina J. Trevino, Ph.D.

Trinity University

Kerry Halladay

Texas Water Resources Institute

The Texas Water Journal is published in cooperation with the Texas Water Resources Institute, part of Texas A&M AgriLife Research, the Texas A&M AgriLife Extension Service, and the College of Agriculture and Life Sciences at Texas A&M University.


**Texas Water
Resources Institute**
make every drop count

Cover photo: Tres Palacios River at FM 1468 near Clemville, Texas. ©2019 Ed Rhodes, TWRI.

As a 501(c)(3) nonprofit organization, the Texas Water Journal needs your support to provide Texas with an open-accessed, peer-reviewed publication that focuses on Texas water. Please consider [donating](#).

Hydrodynamic Modeling Results Showing the Effects of the Luce Bayou Interbasin Transfer on Salinity in Lake Houston, TX

Erik A. Smith^{*a} , Sachin Shah^b 

Abstract: An overreliance on groundwater resources in the Houston (Texas) metropolitan area led to aquifer drawdowns and land subsidence, so regional water suppliers have been turning to surface water resources to meet water demand. Lake Houston, an important water supply reservoir 24 kilometers (15 miles) northeast of downtown Houston, requires new water supply sources to continue to meet water supply demands for the next several decades. The upcoming Luce Bayou Interbasin Transfer Project will divert up to 500 million gallons per day of Trinity River water into Lake Houston. Trinity River water has significantly different water quality than the Lake Houston tributaries. To evaluate the project's potential effect on water quality, the U.S. Geological Survey used an enhanced version of a previously released Lake Houston hydrodynamic model. With a focus on salinity and water-surface elevations, the model combined data from 2009 to 2017 with simulated flow from the Luce Bayou Interbasin Transfer to evaluate potential outcomes from three hypothetical flow scenarios. Overall, these scenarios found that the Luce Bayou Interbasin Transfer would cause salinities to moderately rise over most of the modeled time (2009–2017), although salinities were buffered under 2011 drought conditions. Large inflow events equalized salinities under baseline conditions as well as the enhanced flow scenarios.

Keywords: salinity, hydrodynamic model, water levels, specific conductance

^a Hydrologist, U.S. Geological Survey, Oklahoma-Texas Water Science Center, Geospatial Science/Cyber Innovation Branch, 1451 Green Road, Ann Arbor, MI 48105

^b Hydrologist, U.S. Geological Survey, Oklahoma-Texas Water Science Center, Geospatial Science/Cyber Innovation Branch, 6505 NE 65th Street, Seattle, WA 98115

* Corresponding author: easmith@usgs.gov

Citation: Smith EA, Shah S. 2020. Hydrodynamic modeling results showing the effects of the Luce Bayou Interbasin Transfer on salinity in Lake Houston, TX. *Texas Water Journal*. 11(1):64-88. Available from: <https://doi.org/10.21423/twj.v11i1.7094>.

© 2020 Erik A. Smith, Sachin Shah. This work is licensed under the Creative Commons Attribution 4.0 International License. To view a copy of this license, visit <https://creativecommons.org/licenses/by/4.0/> or visit the TWJ [website](#).

Terms used in paper

| Acronym/Initialism | Descriptive Name |
|--------------------|---|
| ac-ft | acre-feet |
| CRPS | Capers Ridge Pump Station |
| CWA | Coastal Water Authority |
| DWO | Drinking Water Operations |
| EFDC | Environmental Fluid Dynamics Code |
| ft | feet |
| HGSD | Harris-Galveston Subsidence District |
| km | kilometers |
| km ² | square kilometers |
| LBIT | Luce Bayou Interbasin Transfer |
| LBITP | Luce Bayou Interbasin Transfer Project |
| MAE | mean absolute error |
| MGD | million gallons per day |
| mi | miles |
| mi ² | square miles |
| μS/cm | microsiemens per centimeter |
| NRCS | Natural Resources Conservation Service |
| NEWPP | Northeast Water Purification Plant |
| NRMSE | normalized root mean square error |
| NSI | Nash Sutcliffe index of efficiency |
| NWIS | National Water Information System |
| ppt | parts per thousand |
| USGS | U.S. Geological Survey |
| WHCRWA | West Harris County Regional Water Authority |

INTRODUCTION

Houston, Texas will likely soon become the third largest city in the United States ([Eltagouri 2016](#)). The city and surrounding metropolitan area have experienced exponential population growth over the past 70 years. This growth is projected to continue, with the Houston metropolitan area expecting roughly 9.2 million people by 2030 ([WHCRWA 2019](#)). With this population growth, significant pressure has been placed on regional water resources. In 2017 alone, Houston's Drinking Water Operations distributed an average of 449 million gallons per day (MGD; [COH DWO n.d.](#)).

Historically, Houston's water supply demands were largely met by groundwater resources. However, an overreliance on groundwater resources eventually led to the drawdown of regional aquifers ([Gabrysch 1982](#)). The Chicot and Evangeline aquifers, two primary drinking water sources for the region,

had drawdowns of several hundred feet by the mid-1970s ([Gabrysch 1982](#)). In the long run, these drawdowns also led to widespread land subsidence, often as much as 3–4.5 meters (m; 10–15 feet [ft]) across much of the Houston metropolitan area ([Bawden et al. 2012](#); [Kasmarek and Johnson 2013](#)). Because this land subsidence was caused by the permanent compaction of fine-grained aquifer sediments after large-scale groundwater withdrawals, it was recognized that the overreliance on groundwater resources would need to be reversed.

To reduce groundwater usage, regional water suppliers have been gradually switching to surface water resources in compliance with the mandates set by the Harris-Galveston Subsidence District ([HGSD 2020](#)). For the City of Houston (hereinafter referred to as Houston), about 71% of Houston's water supply comes from surface-water resources ([Rendon and Lee 2015](#)), as of 2015. As part of its network of surface-water resources, Houston has partial or complete rights to three reservoirs with

the following daily water supply capacities: Lake Houston (150 MGD; 460 acre-feet [ac-ft]), Lake Conroe (60 MGD; 184 ac-ft), and Lake Livingston (806 MGD; 2,473 ac-ft; [COH DWO 2006](#)). Lake Houston alone supplies 10% to 15% of the total surface-water supply for Houston, according to a published regional water supply map ([COH DWO 2006](#)).

Going forward, a critical component for increasing Houston's drinking water supply is the expansion of the Northeast Water Purification Plant (NEWPP). NEWPP diverts water from Lake Houston, with average daily withdrawal rates of 54 MGD (166 ac-ft) from the 2009 to 2017 period for Lake Houston, based on the daily withdrawal rates included as part of the model archive ([Smith 2019](#)). With the plant expansion set to be completed by 2024, the plant will pull up to an additional 320 MGD (982 ac-ft) from Lake Houston. To meet this extra demand, the City of Houston and the Coastal Water Authority (CWA) have been implementing the Luce Bayou Interbasin Transfer Project (LBITP), a regional water supply project to transfer raw water from the Trinity River to Lake Houston ([CWA n.d.](#)). This project, estimated to be completed in 2020, will divert up to 500 MGD (1,534 ac-ft) of surface water into Lake Houston from the Trinity River.

A growing concern with the LBITP is the potential changes in water quality to Lake Houston. Currently, Lake Houston receives water from seven major tributaries that compose the San Jacinto River Basin ([Sneck-Fahrer et al. 2005](#)). The Trinity River, in contrast, has different water-quality characteristics than the current tributaries flowing into Lake Houston ([Liscum et al. 1999](#); [Liscum and East 2000](#)). For example, the Trinity River generally has higher specific conductance than the Lake Houston tributaries ([Liscum et al. 1999](#); [Liscum and East 2000](#)). This is a concern for municipal and industrial end users that treat raw Lake Houston water via ion exchange plants, as specific conductance is directly correlated with dissolved ionic species. With higher amounts of dissolved ionic species, more effort is required to remove dissolved ions for water treatment processes ([EWT Water Technology 2018](#)). Therefore, large increases in specific conductance can serve as a proxy for estimating changes in water treatment efforts, as the chemical consumption and effluent discharge for processing raw water is directly proportional to the dissolved solids within the raw water.

Beyond potential effects on dissolved ion concentrations, Lake Houston is an important recreational resource for the Houston area. During normal to wet periods, large withdrawals for NEWPP and two regional canals close to the Lake Houston dam do not substantially affect water levels in the lake or affect its recreational use. However, the extended drought in 2011 caused Lake Houston to drop by up to 1.8 m (5.9 ft) and severely reduced the reservoir's recreational capacity ([Brashier 2011](#)). Looking forward, if Lake Houston were to

have increased NEWPP withdrawals and a drought similar to 2011's, the decreases in water levels could become even more problematic with the additional withdrawals ([Combs 2012](#)). As a regional example, a 2012 study commissioned to understand the economic effects of low lake levels on Lake Conroe (Texas) found that low 2011 water levels resulted in decreased revenues from recreational activities and declines in property values ([Rogers et al. 2012](#)).

As the city continues to grow and deal with considerable events ranging from large droughts to catastrophic flooding, such as Hurricane Harvey in 2017, resource planners will need to evaluate how similar events might affect Lake Houston in combination with the new surface-water additions via the LBITP and additional surface-water withdrawals from NEWPP. One method for evaluating how the Luce Bayou Interbasin Transfer (LBIT) inflows and NEWPP withdrawals might affect both the dissolved ion concentrations and water levels of Lake Houston, and under what conditions these effects could be the strongest, is to utilize a hydrodynamic model that can simulate Lake Houston conditions. Hydrodynamic models have been successfully applied in the past to simulate the dynamic hydrology and chemistry of large water bodies such as Lake Houston ([Jin et al. 2007](#); [Dynamic Solutions 2013](#)). In 2015, the U.S. Geological Survey developed such a tool, a three-dimensional circulation, temperature, and salinity transport model for Lake Houston ([Rendon and Lee 2015](#)) using the Environmental Fluid Dynamics Code (EFDC) modeling package ([Hamrick 1992](#); [Hamrick 1996](#)). As this model also simulates salinity, the salinity can be related back to specific conductance and therefore can be used as an evaluation tool for changes in dissolved ion concentrations.

However, the original EFDC hydrodynamic model developed for Lake Houston ([Rendon and Lee 2015](#)) did not account for the proposed LBIT flows or the additional NEWPP withdrawals. Furthermore, the existing Lake Houston EFDC model was originally calibrated and verified for only a 2-year period: 2009–2010. To improve the original model's scope, the USGS, in cooperation with the ExxonMobil Corporation, expanded the model's capabilities to evaluate both the LBITP flows and NEWPP withdrawals on Lake Houston across a wide range of hydrological and climatological conditions. These hypothetical scenarios were designed to investigate the potential effects of the LBITP on both water levels and salinity ranges under historical conditions as a proxy for future conditions. As of 2020, the ExxonMobil Baytown Complex is one of the largest industrial end users of raw Lake Houston water and therefore has a vested interest in the future water quality of Lake Houston. The expanded model looked across almost a decade of hydrological and climatological conditions, simulating water-surface elevations, water temperature, and salinities from 2009 to 2017. This expanded period contained both an extended drought (2011) and several large flooding events (2016 and 2017).

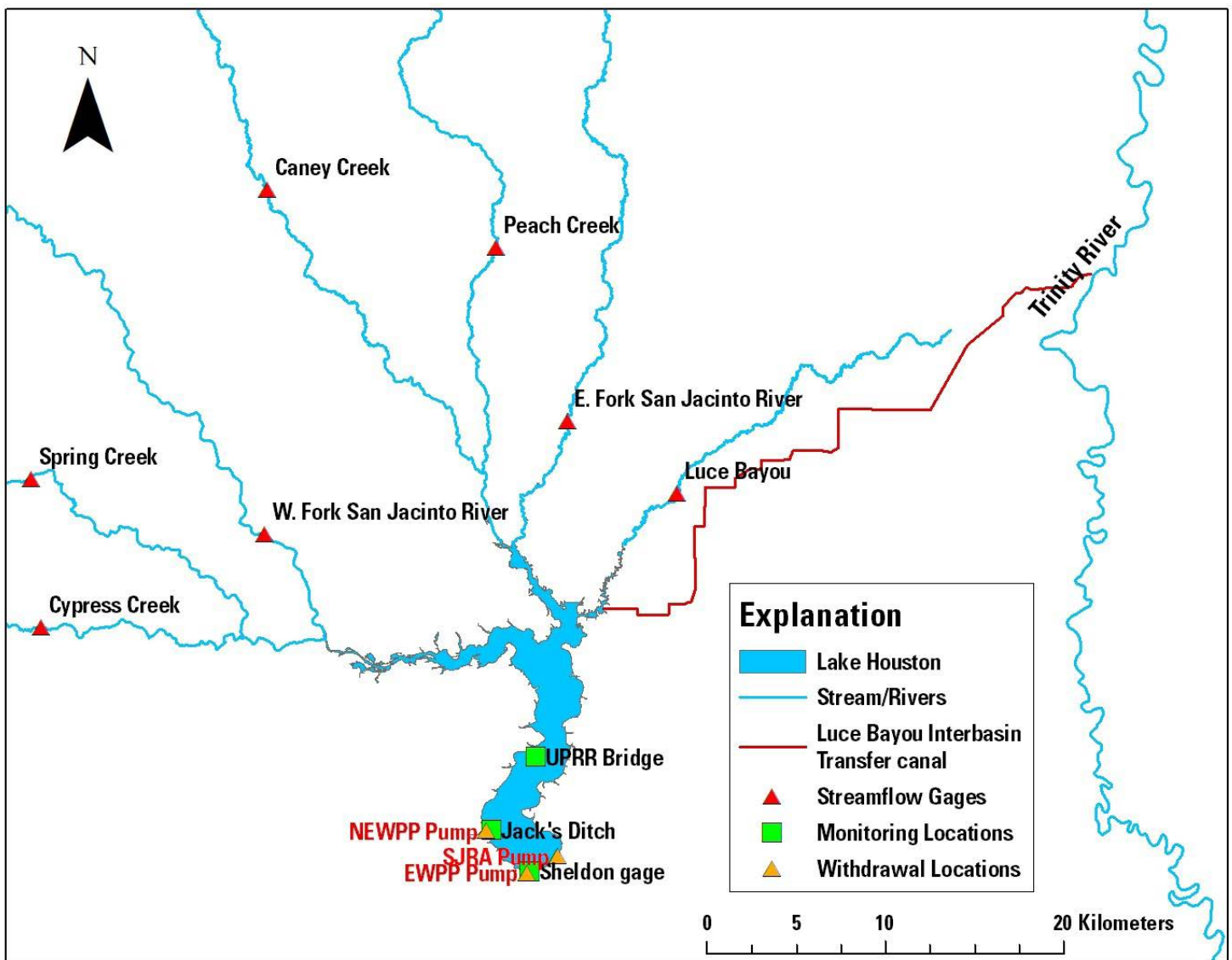


Figure 1. Map of Lake Houston, streams and rivers, streamgages, monitoring locations, withdrawal locations, and the Luce Bayou Interbasin Transfer Canal.

Luce Bayou Interbasin Transfer

Lake Houston has a storage capacity of approximately 47,800 million gallons (146,700 ac-ft; [Rendon and Lee 2015](#)). Once the LBITP is fully operational, the LBITP would equal approximately 1.0% of the daily total Lake Houston capacity at 500 MGD (1,534 ac-ft). The LBITP will also allow NEWPP to meet its required mandate to convert to primarily surface-water sources. The CWA will start actively transferring water sometime in 2020 ([CWA 2019](#)) at the Capers Ridge Pump Station (CRPS) located on the Trinity River (Figure 1). The CRPS pumps water into a series of large pipelines that convey the water for approximately 4.8 kilometers (km; 3 miles

[mi]) before outflowing into a sedimentation basin at the start of a 37.8-km (23.5 mi) earthen canal ([AECOM 2011](#)). Trinity River water will be introduced via the northeast corner of Lake Houston near Luce Bayou and allowed to mix with lake water.

Currently, the maximum flow for the LBITP once in operation is 12.6 cubic meters per second (445 cubic feet per second), or 240 MGD (737 ac-ft), based on the installation of four pumps at CRPS ([Miller and Marks 2018](#)). Eventually, the LBIT is expected to sustain flows of 240 MGD or more after the first couple of years of operation. Although the additional pumps are not set up to pump 500 MGD (1,534 ac-ft), the structures are in place to add capacity up to the permitted limit of 500 MGD.

Table 1. Gaged watershed area, watershed subdivision (eastern or western), and applied scaling factor for estimating the inflows from all tributaries to Lake Houston, near Houston, Texas during model runs from 2009 to 2017. [U.S. Geological Survey, USGS; km², square kilometers; mi², square miles]

| USGS station number | USGS station name | Short name in Figure 1 | Eastern or western watershed | Watershed area (km ² [mi ²]) | Scaling factor (K) |
|---------------------|---|---------------------------|------------------------------|---|--------------------|
| 08069000 | Cypress Creek near Westfield, Texas | Cypress Creek | Western | 727.8 (281.0) | 1.15 |
| 08068500 | Spring Creek near Spring, Texas | Spring Creek | Western | 1051 (405.7) | 1.11 |
| 08068090 | West Fork San Jacinto River above Lake Houston near Porter, Texas | W. Fork San Jacinto River | Western | 2527 (975.5) | 1.05 |
| 08070500 | Caney Creek near Splendora, Texas | Caney Creek | Eastern | 272.7 (105.3) | 2.12 |
| 08071000 | Peach Creek at Splendora, Texas | Peach Creek | Eastern | 306.4 (118.3) | 1.37 |
| 08070200 | East Fork San Jacinto River near New Caney, Texas | E. Fork San Jacinto River | Eastern | 1004 (387.7) | 1.07 |
| 08071280 | Luce Bayou above Lake Houston near Huffman, Texas | Luce Bayou | Eastern | 396.8 (153.2) | 1.14 |

STUDY SITE

Lake Houston (Figure 1) is a man-made reservoir about 24 km (15 mi) northeast of downtown Houston, Texas. The Lake Houston Dam, constructed between 1951 and 1953, impounds the West and East Forks of the San Jacinto River and serves as the primary municipal water supply for Houston, Texas (TWDB n.d.). Lake Houston also serves as a major water resource for industrial, commercial, and agricultural irrigation customers, as well as other regional municipalities. Seven major tributaries flow into Lake Houston that drain the San Jacinto River basin upstream from Lake Houston. Generally, these tributaries are grouped into one of two major subbasins: a western and eastern subbasin, comprising the West and East Forks of the San Jacinto River, respectively (Sneck-Fahrer et al. 2005). The western subbasin tributaries include Cypress Creek, Spring Creek, and West Fork San Jacinto River (Table 1). The eastern subbasin tributaries include Caney Creek, Peach Creek, East Fork San Jacinto River, and Luce Bayou (Table 1).

The regional climate for the Lake Houston watershed is classified as humid subtropical, with a mean precipitation of 1.28 m (4.2 ft) per year between 2008 and 2017, based on the Global Summary of the Year from 2008 to 2018 for George Bush Intercontinental Airport (<https://gis.ncdc.noaa.gov/maps/ncei/cdo/annual>). Due to periodic thunderstorms, sustained rainfall, and occasional hurricanes, the area is prone to flooding. Climate in the region has also been known to experience sustained drought periods, which can have a profound effect on lake level.

The lake has a capacity of about 181.0 million cubic meters (6.391 billion cubic feet; 146,700 ac-ft) and a surface area of 49.5 square kilometers (km²; 19.1 square miles [mi²]; Rendon and Lee 2015). Mean depth at capacity of Lake Houston is about 3.7 m (12 ft) and the maximum depth is about 15.2

m (50 ft; Liscum and East 2000). Lake Houston drainage basin is approximately 7,213 km² (2,785 mi²). The USGS is continuously collecting data at two locations in Lake Houston: Lake Houston south of Union Pacific Bridge near Houston, Texas (USGS 295826095082200; hereafter referred to as UPRR Bridge) and Lake Houston at the mouth of Jack's Ditch near Houston, Texas (USGS 295554095093401 or USGS 295554095093402; hereafter referred to as Jack's Ditch; Buessink and Burnich 2009). Both locations continuously collected the following data on an hourly basis using a multi-probe sonde on a multi-depth monitoring buoy for at least part of the 2009–2017 period: dissolved oxygen, turbidity, specific conductance, water temperature, and pH. Data for these locations are available using the USGS station numbers (USGS 2020).

METHODS

A previously developed three-dimensional hydrodynamic model of Lake Houston was used as the starting version for the enhanced Lake Houston model. The original Lake Houston model was used to simulate three-dimensional circulation, water temperature, salinity, and residence time (Rendon and Lee 2015). Both the original and enhanced models were developed with EFDC, a grid-based surface-water modeling package developed for estuarine and coastal applications (Hamrick 1992; Hamrick 1996). EFDC solves the vertically hydrostatic equations for turbulent flow for a variable-density fluid (including salinity and temperature dependencies). EFDC is a widely used modeling framework that has been applied in a variety of surface-water studies (Ji 2017), including several reservoirs throughout the southern United States (Ji et al. 2004; Elçi et al. 2007; Dynamic Solutions 2013).

The EFDC model structure used in this study required bathymetric data, bottom friction coefficients, tributary inflow loca-

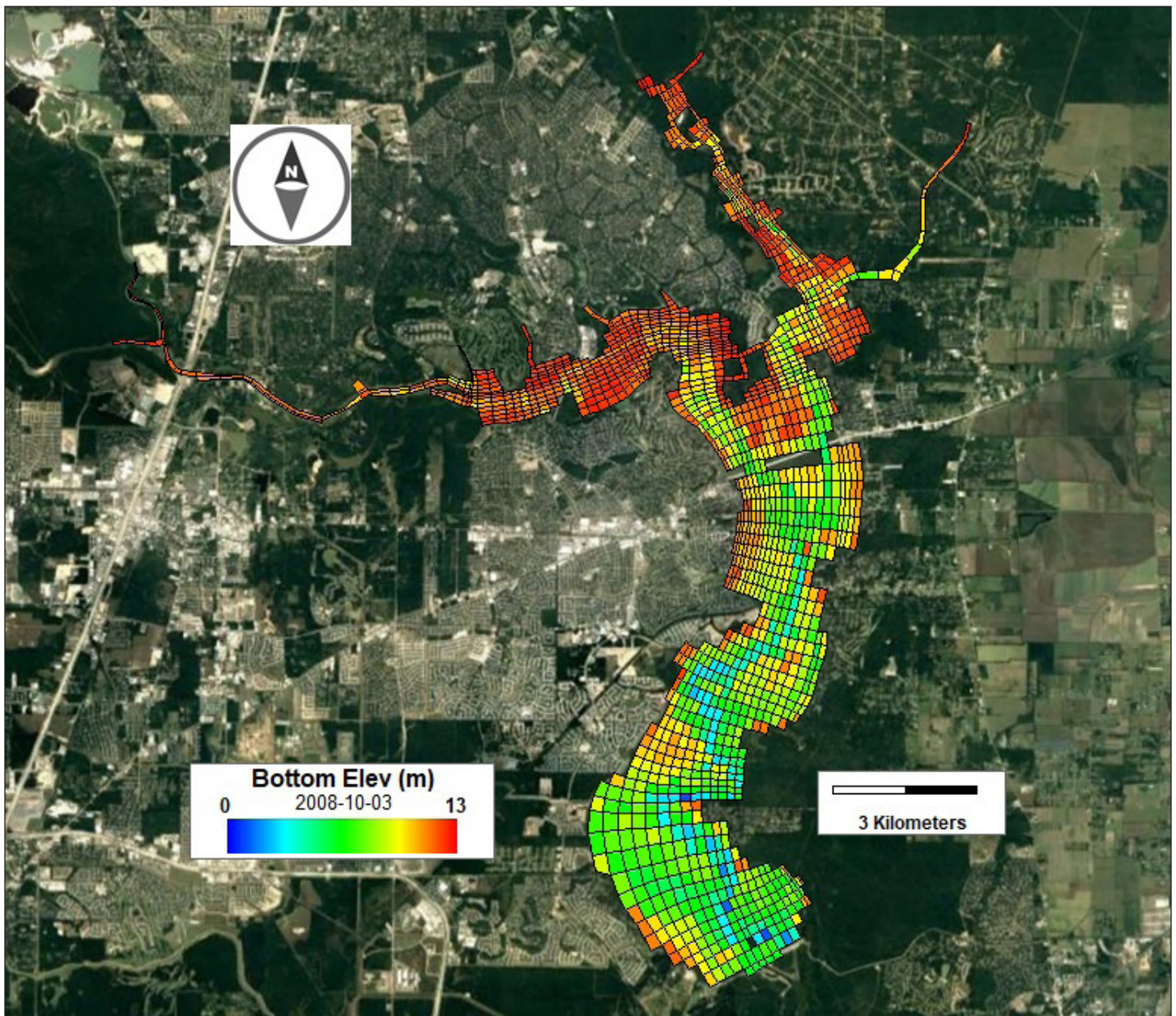


Figure 2. Model domain for the Lake Houston EFDC model, showing the two-dimensional layout of grid cells with the color scale denoting the bottom elevation of the grid cell (in meters).

tions, withdrawal locations (i.e., water intake pumping stations, canal diversions), and any hydraulic structures in the model domain (i.e., the dimensions of the dam impounding Lake Houston). Except for adding the LBIT to the model domain, the original Lake Houston EFDC model structure (Rendon and Lee 2015) was preserved for the updated model (Figure 2). For all aspects of running the EFDC model, EFDC_Explorer version 8.4 (compiled 2018-07-23) was selected, a graphical user interface pre- and post-processor for EFDC models (Craig 2017). EFDC_Explorer was used to enter the required input data into the EFDC model, control model parameters,

manipulate run-time configurations, initiate model runs, and perform post-run statistical comparisons.

The enhanced model was recalibrated for the period 2009–2011 and validated for the period 2012–2017 (Smith 2019). Several continuous flow and water-quality monitoring datasets were used to calculate the initial and boundary conditions for the Lake Houston model and to provide calibration data. Data characterizing Lake Houston hydrologic conditions and its contributing areas were compiled for this effort, including inflow from all seven tributaries to Lake Houston and water-surface elevation from Lake Houston near Sheldon, Texas (USGS 08072000; hereafter referred to as Sheldon gage).

Other compiled data included specific conductance and water temperature from a subset of the gaged inflow locations, in addition to specific conductance and water temperature from the two Lake Houston monitoring stations.

Streamflow data collection and water-surface elevations

Streamflow was continuously measured for the seven major tributaries to Lake Houston. Finalized continuous streamflow records used in the enhanced Lake Houston EFDC model development are available from the USGS National Water Information System (NWIS) database using the station numbers provided in Table 1 (USGS 2020) for seven streamgage locations upstream from Lake Houston (Figure 1; Table 1). As part of the continuous streamflow record development, instantaneous discharge and stage measurements were periodically performed at these streamgage locations to verify and modify the stage-discharge relation (Rantz 1982; Mueller et al. 2013). Measured water-surface elevations for calibrating and verifying the EFDC simulations were from Sheldon gage; data are available using USGS station number 08072000 (USGS 2020).

Watershed areas for the seven major tributary locations were delineated in ArcGIS (ESRI 2018) using watershed boundary datasets available from the USGS and U.S. Department of Agriculture, Natural Resources Conservation Service (USGS and USDA NRCS 2013). A percentage of each watershed was considered to have ungaged inflow, as it was determined to not contribute to the flow measured by the USGS streamgage. To consider this flow into the model domain, a variation of the rational method described by Chow et al. (1988) and applied by Rendon and Lee (2015) for the original Lake Houston EFDC model was used. A scaling factor (K) was calculated separately for each watershed that related the ungaged watershed area to the gaged watershed area in order to estimate the total contributed flow from each major tributary (Equation 1):

$$K = 1 + \frac{A_{utw}}{A_{gtw}} + \frac{A_{ul}}{A_{gl}} \quad (1)$$

where

- A_{utw} is the ungaged tributary watershed area, in square kilometers;
- A_{gtw} is the gaged tributary watershed area, in square kilometers;
- A_{ul} is the ungaged lake watershed area, in square kilometers; and,
- A_{gl} is the gaged lake watershed area, in square kilometers.

Additionally, Lake Houston inflows also were attributed to other ungaged locations outside of the seven major tributaries, accounting for approximately 3.3% of total area. This additional inflow was also accounted for in the EFDC model (Smith 2019).

Withdrawals from Lake Houston

Three major withdrawals were accounted for in both versions of the Lake Houston EFDC model (Figure 1). Close to Jack's Ditch (Figure 1), pump 1 withdraws water for one of Houston's three primary water treatment facilities. Daily withdrawals typically range from 20 to 80 MGD, with a mean daily withdrawal rate of 54 MGD over the 2009–2017 period. On the west side of the Lake Houston dam, pump 2 withdraws water for the canal that conveys water to the south and west of Lake Houston. Daily withdrawals typically range from 17 to 120 MGD (52 to 368 ac-ft), with a mean daily withdrawal rate of 42 MGD (129 ac-ft) over the 2009–2017 period, based on the full withdrawal rates included as part of the model archive (Smith 2019). Along the east side of the Lake Houston dam, pump 3 withdraws water for the canal that conveys water to the south and east of Lake Houston. Daily withdrawals typically range from 11 to 94 MGD (34 to 288 ac-ft), with a mean daily withdrawal rate of 48 MGD (147 ac-ft) over the 2009–2017 period, based on the full withdrawal rates included as part of the model archive (Smith 2019).

Water temperature and specific conductance

Continuous daily water temperature was available (2009–2017; USGS 2020) for two of the seven major tributaries: Spring Creek near Spring, Texas (USGS 08068500) and East Fork San Jacinto River near New Caney, Texas (USGS 08070200). Each input tributary required a temperature assignment in the model, so Spring Creek measurements were applied to the western watersheds and East Fork San Jacinto River measurements were applied to the eastern watersheds (Table 1). Within Lake Houston, continuous water temperature was measured hourly at two locations (Figure 1): UPRR Bridge and Jack's Ditch (USGS 2020).

Each of the seven tributaries required a salinity estimate for the inflows. As mentioned earlier, direct measurements of salinity were not available, so available specific conductance (in microsiemens per centimeter, or $\mu\text{S}/\text{cm}$) records were converted to salinity (in parts per thousand, or ppt). Continuous specific conductance records were available (USGS 2020) for all or part of the 2009–2017 period for four of the seven major tributaries (Table 1): Spring Creek near Spring, Texas (USGS 08068500), East Fork San Jacinto River near New Caney, Texas (USGS 08070200), Cypress Creek near Westfield, Texas (USGS 08069000), and West Fork San Jacinto River near Humble, Texas (USGS 08069500).

Except for the East Fork San Jacinto River, the salinity record for the other six tributaries were either derived from a mathematical relation or a combination of a relation to discharge and direct measurements (Table 2). Using the same methods as

Table 2. Watershed names for each tributary into the Lake Houston EFDC model, the Equation 2 constants and coefficients of determination (R²), the U.S. Geological Survey streamgage station name for the streamflow/salinity relation, and the assignment methods for salinity inputs into the enhanced Lake Houston EFDC model. [U.S. Geological Survey, USGS; ---, not applicable]

| Watershed name | Constants and R ² (a and b constant from eq. 1, R ² in parentheses) | USGS station name for streamflow/salinity relation | Assignment of tributary salinity input |
|-----------------------------|---|---|--|
| West Fork San Jacinto River | 0.3928, 0.343 (0.74) | West Fork San Jacinto River near Humble, Texas (USGS 08069500) | West Fork relation: 10/03/2008–5/18/2010, 01/30/2011–10/30/2013; West Fork, direct measurements: 5/18/2010–12/31/2010, 10/30/2013–12/31/2017 |
| Spring Creek | 0.2506, 0.385 (0.86) | Spring Creek near Spring, Texas (USGS 08068500) | Spring Creek relation |
| Cypress Creek | 0.3623, 0.444 (0.61) | Cypress Creek near Westfield, Texas (USGS 08069000) | Cypress Creek relation |
| East Fork San Jacinto River | 0.085, 0.25 (0.40) | East Fork San Jacinto River near New Caney, Texas (USGS 08060200) | East Fork San Jacinto, direct measurements |
| Caney Creek | --- | --- | East Fork San Jacinto River relation |
| Peach Creek | --- | --- | East Fork San Jacinto River relation |
| Luce Bayou | --- | --- | East Fork San Jacinto River relation |

Rendon and Lee (2015), the following mathematical relation between streamflow and salinity was used (Equation 2):

$$S = a \times Q^{-b} \tag{2}$$

where

- S* is salinity, in parts per thousand;
- a*, *b* are curve-fitting coefficients; and,
- Q* is instantaneous streamflow for the individual watershed, in cubic meters per second.

Table 2 shows the curve-fitting coefficients, if a streamflow to salinity relation was done for the individual watershed; in parentheses, coefficient of determination (R²) values (Helsel and Hirsch 2002) for the streamflow-salinity relation are shown. Table 2 also shows how each individual watershed’s salinity record was assigned throughout the entire calibration and verification record. Because these were indirect relations, it should be noted that the methodology used to estimate salinity may not fully characterize each inflow. Table 2 highlights the uncertainty, particularly for the eastern subbasin watersheds; overall, the East Fork San Jacinto River relation was the best surrogate available for assigning salinity for these tributaries.

As with the streamflow data, the continuous water temperature and specific conductance data are available from the USGS NWIS database (USGS 2020). Calibration datasets for specific conductance, converted to salinity, were available for the same period and frequency as water temperatures at UPRR

Bridge and Jack’s Ditch. Salinity (in ppt) was transformed from specific conductance (in μS/cm) through a general equation and rating table (Wagner et al. 2006).

The expected salinity changes for Lake Houston due to the new LBIT flow are one of the primary goals for the new modeling scenarios. However, there was no continuous record available for either salinity or specific conductance for the Trinity River water near the CRPS. Because the EFDC model required an input salinity record (converted from specific conductance) for the LBIT, it was necessary to evaluate the best surrogate available for the LBIT. For purposes of modeling LBIT for the modeling periods from 2009 to 2017, the continuous specific conductance record from the CWA canal at Thompson Road near Baytown, Texas (USGS 08067074; USGS 2020; not shown) was used. This record represents Trinity River water that has been diverted into a CWA canal approximately 35 km downstream from Capers Ridge. Based on comparisons of data from USGS synoptic sampling locations for the Trinity River south of Lake Livingston to the CWA canal record, it was found that the synoptic data had the same general trends and ranges of specific conductance where it and the CWA canal record overlapped. Therefore, the CWA canal continuous record was deemed an appropriate surrogate for LBIT. However, prior to August 2012, the long-term average specific conductance for all the available CWA canal data of 357 μS/cm (converted to salinity; 0.164 ppt) was used because the continuous CWA canal record did not exist.

Table 3. Model parameterization differences between the original Lake Houston EFDC model (Rendon and Lee 2015) and the enhanced model.

| Parameter | Description | Rendon and Lee (2015) | Enhanced model | Variation range | Variation comment |
|-----------|--|------------------------------|----------------------------------|-------------------|-------------------------|
| FSWRATF | Minimum fraction adsorbed in the top layer | 0.30 | 0.45 | 0.2–0.6 | Sensitive |
| WQKEB | Background light extinction, (m ⁻¹) | 1.6 | 2.3 | 1.2–2.5 | Sensitive |
| IGRIDV | Selection of grid type: standard sigma versus sigma-zed layering | Standard sigma vertical grid | Sigma-zed vertical layering grid | N/A | Sensitive |
| SGZmin | Minimum number of sigma-zed layers | N/A | 3 | 3–5 | Insensitive |
| DTSSDHDT | Dynamic time stepping rate of depth change | 0 | 0.15 | 0–0.3 | Model run stabilization |
| NUPSTEP | Minimum number of iterations for each time step | 2 | 4 | 2–6 | Model run stabilization |
| DTMAX | Maximum time step for dynamic stepping (in seconds) | 50 | 100 | 25–125 | Model run stabilization |
| ABO | Vertical molecular diffusivity | 1 E-09 | 1 E-06 | 1 E-05– 1 E-09 | Insensitive |

Meteorological data

Hourly values for selected meteorological data from 2009 through 2017 (dry bulb temperature [air temperature], relative humidity, air pressure, precipitation, cloud cover, wind speed, and wind direction) were measured at two different locations. For 2009 through March 2010, hourly data from the National Weather Service meteorological station at George Bush Intercontinental Airport was used (<https://www.ncdc.noaa.gov/cdo-web/>). Starting after April 8, 2010, the USGS weather station located at the Sheldon gage, near the southern end of Lake Houston, was used, and the data used is available as part of the model archive (Smith 2019). Evaporation was calculated internally in the EFDC model, based on the aerodynamic method of calculating evaporation from an open body of water (Chow et al. 1988).

Model parameterization

Most of the EFDC parameters that control the grid, bottom roughness, hydraulic boundary conditions, model run timing, and heat exchange were the same between the original Lake Houston EFDC model (Rendon and Lee 2015) and the new enhanced EFDC model. A few key differences related to time-step control, grid type, light extinction conditions, and the surface heat exchange submodel did exist between the two versions, as shown in Table 3. These parameters were varied by trial and error through a series of calibration model runs to improve the overall fit of the model.

The selection of the water balance evapotranspiration model (EFDC Original) was left the same, but the underlying surface heat exchange submodel parameterization was adjust-

ed. Two parameters within the surface heat exchange model, FSWRAFT and WQKEB (Table 3), were found to be sensitive, particularly for the water-surface elevation calibration. Also, changing the selected grid type (IGRIDV) from standard sigma vertical layering to sigma-zed vertical layering made for a better water-surface elevation fit (Craig 2017). Finally, a series of parameters that control the model run timing (DTSSDHDT, NUPSTEP, DTMAX), and one parameter that affects the hydrodynamics (ABO), were adjusted to help with model run stabilization but were relatively insensitive for improving the model calibration.

The hydraulic structure data, as stored in the free surface elevation control file, was adjusted to account for new rating curve measurements available since the 2015 model publication. In particular, the adjusted rating curve accounted for the high flows observed during the 2016 and 2017 flooding events. The overall hydraulic structure setup, such as the length of the model cells that encompass the Lake Houston Dam, was unaltered from the original model.

RESULTS

Calibration and verification of the enhanced model

The enhanced Lake Houston EFDC model was modified and calibrated by using input boundary conditions from 2009 through 2011. The model was then verified by using 2012 through 2017 input boundary conditions as a secondary performance test. Model results at three locations in the model grid of Lake Houston (at various depths) were compared to measured data collected from the three data collection sites on the lake (Figure 1). The three types of data used to verify model

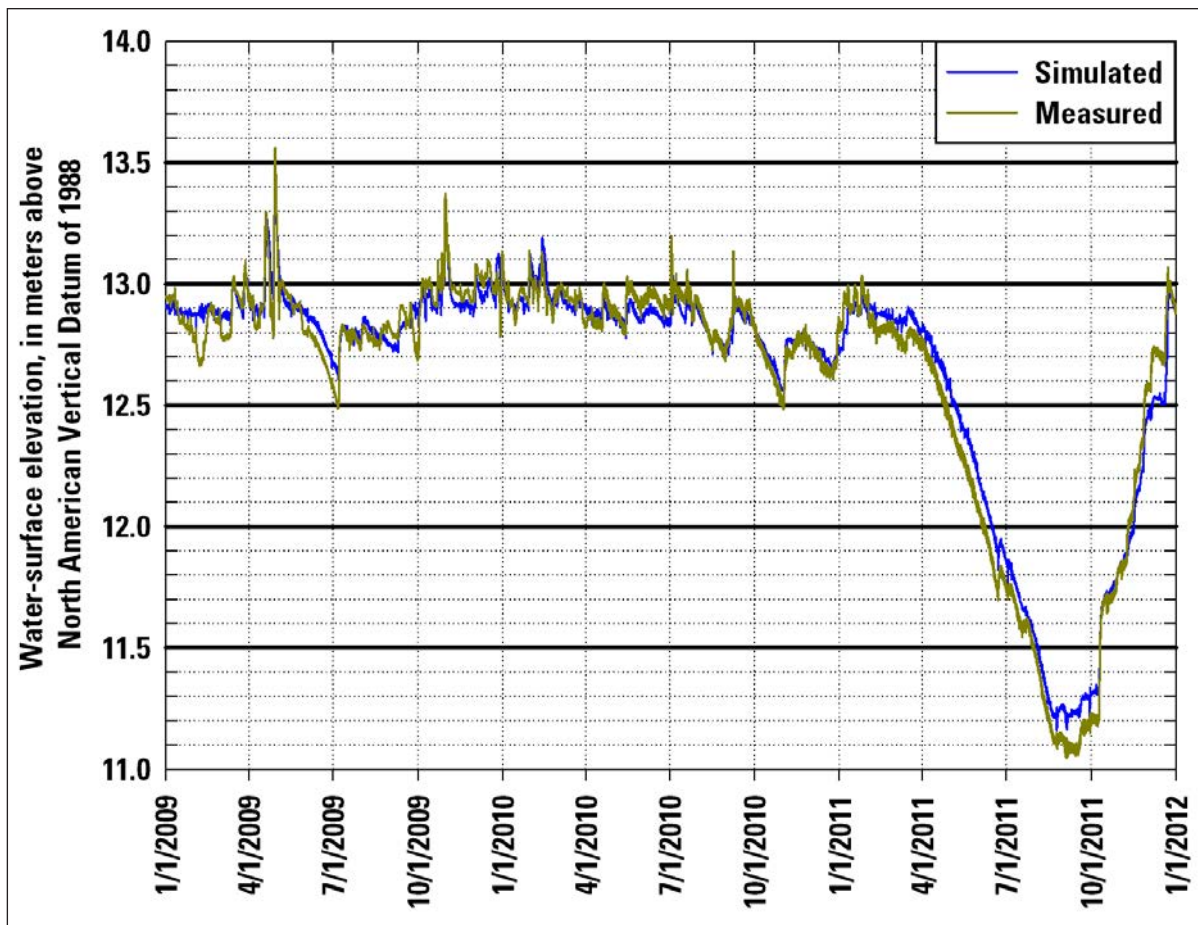


Figure 3. Simulated and measured water-surface elevations, in meters above the North American Vertical Datum of 1988 (NAV88), for Lake Houston, 2009–2011.

performance were water-surface elevations, salinity (computed from measured specific conductance), and water temperature. Water-surface elevations were compared at the Sheldon gage. Salinity and water temperature were compared at the two lake locations: UPRR Bridge and Jack's Ditch. For both UPRR Bridge and Jack's Ditch, continuous records were available at four different depths: 0.3 m (1.0 ft), 1.8 m (5.9 ft), 3.7 m (12.1 ft), and 4.9 m (16.1 ft). Not all the datasets were complete, particularly for the UPRR Bridge. Only the continuous record for the 0.3-m (1.0-ft) depth continued after June 2010 for the UPRR Bridge; on the other hand, most of the Jack's Ditch records for all four depths were nearly complete (2009–2017). Overall, adequate datasets existed for comparison during both the calibration and verification periods.

Three statistics were used to evaluate performance of the Lake Houston EFDC model: mean absolute error (MAE), normalized root mean square error (NRMSE), and the Nash-Sutcliffe index of efficiency (NSI; [Nash and Sutcliffe 1970](#)). The MAE is a goodness-of-fit statistic calculated as the mean of the absolute differences between the simulated (model) value and the measured value ([Legates and McCabe 1999](#)). The NRMSE is

a slightly different metric, calculated as the root of the mean of the squares of the difference between the simulated and measured values, then divided by the range of measured values to remove the units of measure (dimensionless). The last goodness-of-fit statistic, the NSI has been classically used to evaluate hydrological model performance ([Legates and McCabe 1999](#)). The NSI ranges from minus infinity to positive 1.0: Any value above 0.0 indicates that the model is a better predictor of the measured data than the mean of the measured data, with 1.0 indicating a perfect match. NSI values below 0.0 indicate the model is worse than the mean of the measured data. For the exact NSI formula, also termed the coefficient of efficiency, consult Nash and Sutcliffe ([1970](#)) or Legates and McCabe ([1999](#)).

The first step in the calibration process for this revised Lake Houston model was the water balance. Before the water temperature and salinity calibrations could proceed, the differences between the simulated and measured water-surface elevations were resolved. The final calibrated model was able to replicate most of the large inflow events as well as accurately simulate the large drought event in 2011. A comparison between the

Table 4. Performance evaluation statistics for the enhanced 2019 Lake Houston EFDC model. Summary for the following evaluation criteria: simulated water-surface elevation relative to measured water-surface elevation, simulated salinity relative to salinity computed from specific conductance, and simulated water temperature relative to measured water temperature. Criteria represent the range of values for the individual depths (0.3 m [1.0 ft], 1.8 m [5.9 ft], 3.7 m [12.1 ft], 4.9 m [16.1 ft]) at U.S. Geological Survey reservoir stations Lake Houston south of Union Pacific Railroad Bridge near Houston, Texas (USGS 295826095082200) and Lake Houston at the mouth of Jack's Ditch near Houston, Texas (USGS 295554095093401; [USGS 2020](#)). [m, meters; ft, feet; ppt, parts per thousand; °C, degrees Celsius; MAE, mean absolute error; NRMSE, normalized root mean square error; NSI, Nash Sutcliffe index of efficiency]

| Year(s) | Evaluation Criteria | | |
|-------------------------|---------------------|-----------|-----------|
| | MAE | NRMSE | NSI |
| Water-surface elevation | | | |
| 2009–2011 | 0.06 m (0.20 ft) | 0.03 | 0.98 |
| 2012–2017 | 0.05 m (0.16 ft) | 0.02 | 0.85 |
| Salinity | | | |
| 2009–2011 | 0.007–0.009 ppt | 0.05–0.09 | 0.84–0.97 |
| 2012–2017 | 0.007–0.009 ppt | 0.05–0.06 | 0.80–0.94 |
| Water temperature | | | |
| 2009–2011 | 0.66–0.86 °C | 0.03–0.04 | 0.98 |
| 2012–2017 | 0.75–0.92 °C | 0.03–0.04 | 0.97–0.98 |

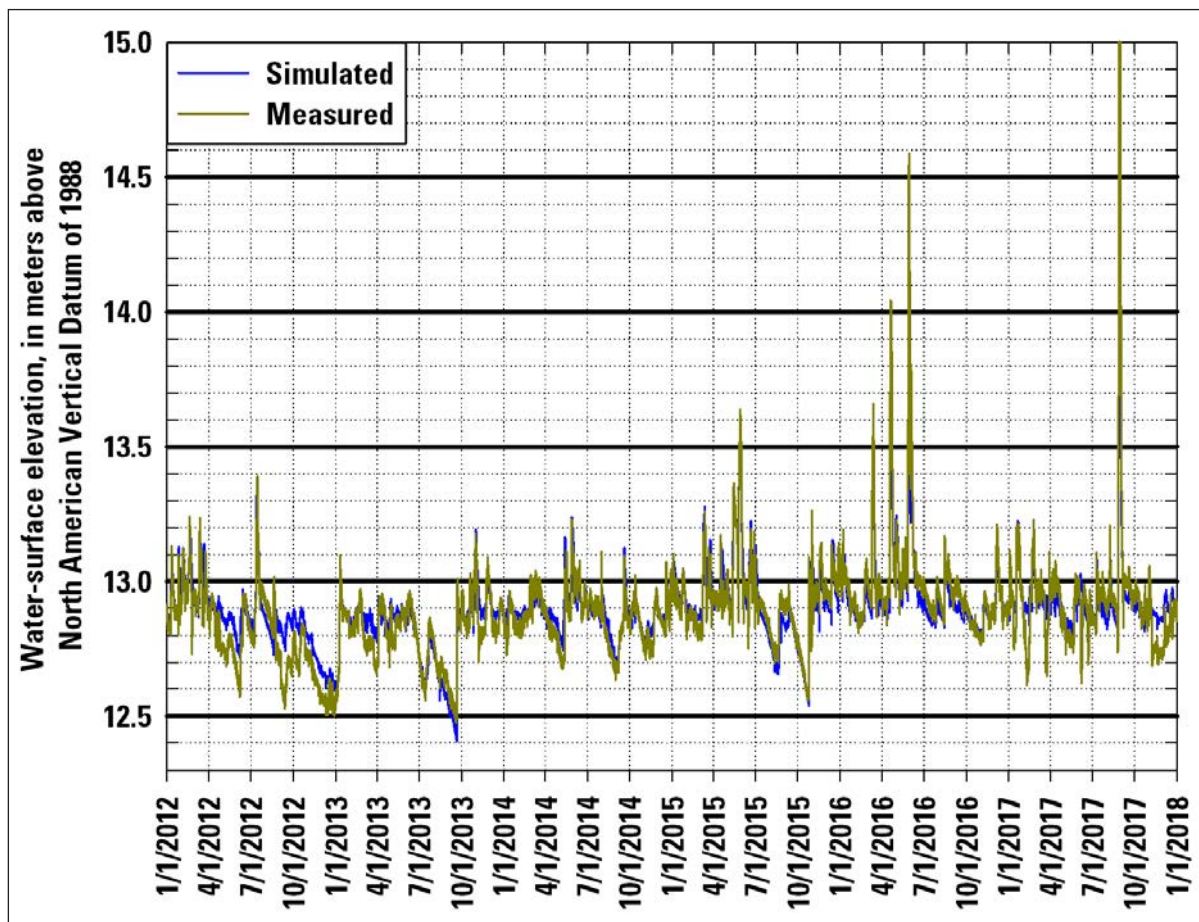


Figure 4. Simulated and measured water-surface elevations, in meters above the North American Vertical Datum of 1988 (NAV88), for Lake Houston, 2012–2017.

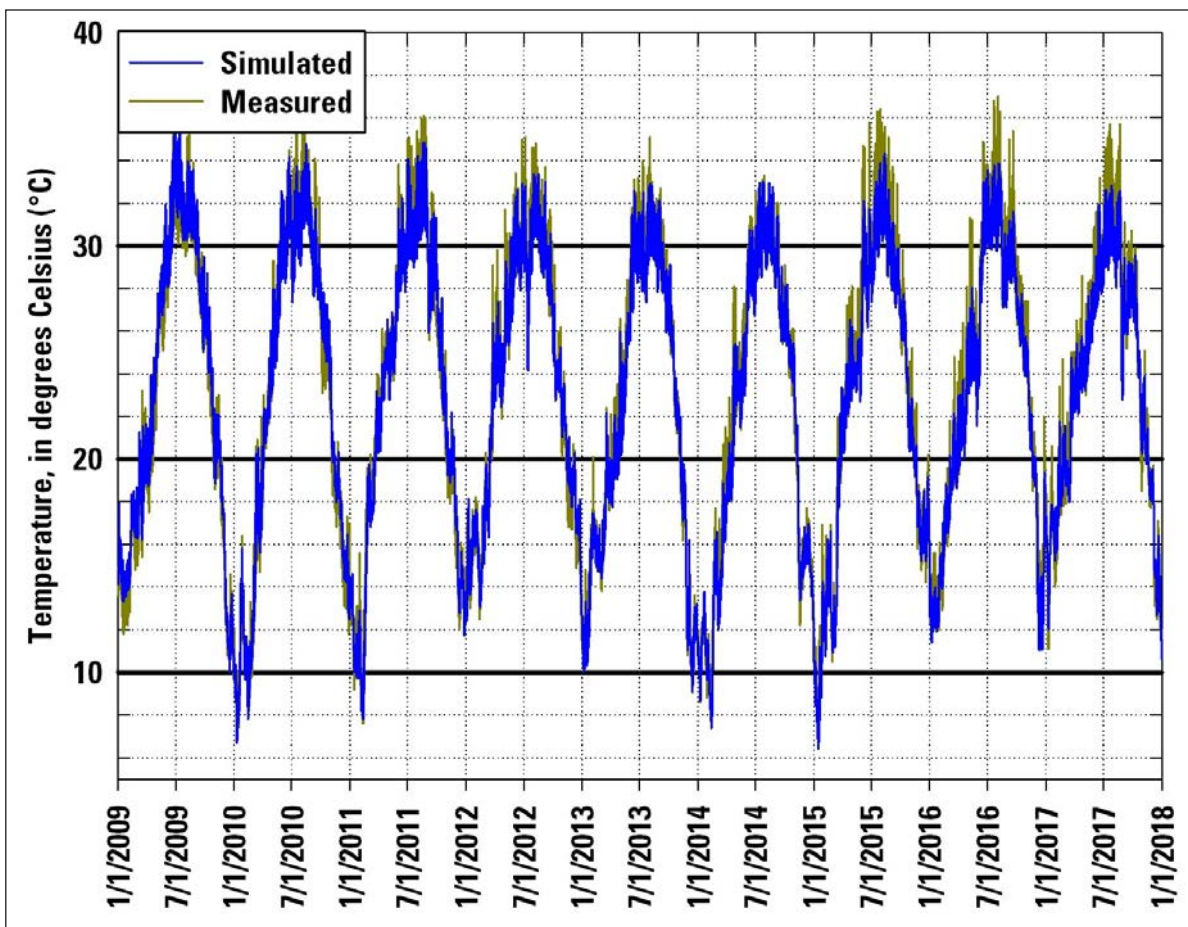


Figure 5. Simulated and measured temperature, in degrees Celsius, at 0.3-meter (1-foot) depth for Lake Houston south of Union Pacific Railroad Bridge near Houston, Texas (USGS 295826095082200), 2009–2017.

simulated and measured water-surface elevations for Lake Houston is shown in Figure 3. Overall, the enhanced Lake Houston EFDC model had an improved model fit to the measured water-surface elevation data for the three goodness-of-fit statistics selected over the original model (Rendon and Lee 2015). Table 4 shows the primary statistics for the calibration from 2009 to 2011 and the verified period from 2012 to 2017 (Figure 4). The MAE and NRMSE values were generally one-half of the original model for water-surface elevation, with an NSI of 0.98 for the calibration (2009–2011) and 0.85 for the verification period (2012–2017). For comparison, the original model had an NSI of 0.54 for the selected calibration year (2009) and 0.75 for the validation year (2010).

Water temperature for the enhanced model had NSI values above 0.9, similar to Rendon and Lee (2015) NSI values. The simulated temperatures effectively tracked the measured data across all four depths. MAE values for the enhanced model were generally between 0.6 and 0.9 °C (0.54 to 1.62 °F) for all depths. Overall, the model matched the measured data very closely for water temperature, as shown in Figure 5 at 0.3-m (1-ft) depth for the UPRR Bridge.

Figure 6 shows the simulated and measured salinity (converted from specific conductance) for the 2009–2017 period at 0.3-m (1-ft) depth for the UPRR Bridge. As with temperature, all four depths generally showed the same pattern with only slight variations with depth for salinity. Salinity had MAE values ranging from 0.007 to 0.009 ppt for the calibration, NRMSE values ranging from 0.04 to 0.09, and NSI values ranging from 0.83 to 0.97. For the verification period (2012–2017), salinity had MAE values ranging from 0.007 to 0.009 ppt for the calibration, NRMSE values ranging from 0.05 to 0.06, and NSI values ranging from 0.80 to 0.94. Overall, the simulated salinity values were able to adequately replicate most of the large inflow events and most importantly, simulate the high salinity values during the 2011 drought. Also, the NSI values exceeded the original model calibration and validation, which ranged from 0.66 to 0.86 (Rendon and Lee 2015).

Long-term LBIT simulations

A series of three model scenarios were run to better understand the long-term water-surface elevation and salinity effects

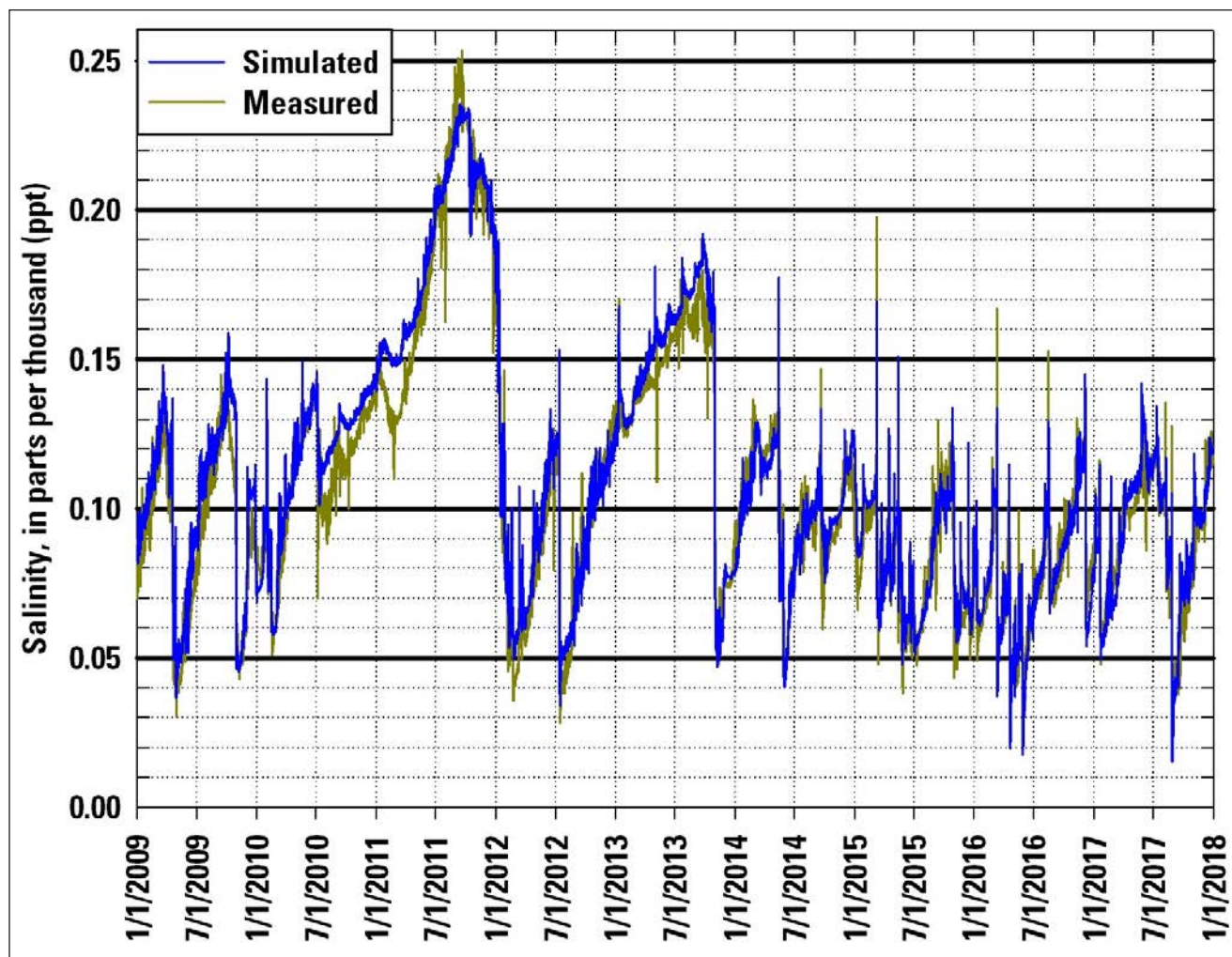


Figure 6. Simulated and measured salinity, in parts per thousand (ppt), at 0.3-meter (1-foot) depth for Lake Houston south of Union Pacific Railroad Bridge near Houston, Texas (USGS 295826095082200), 2009–2017.

of sustained pumping of Trinity River water through the LBIT to Lake Houston. All three LBIT scenarios spanned the entire period from 2009 to 2017. Running the model for the entire period was done to evaluate how the proposed sustained pumping under the LBIT would have affected Lake Houston under the hydrological and climatological conditions for the period of record. In all three simulations, it was assumed an additional 320 MGD (982 ac-ft) were withdrawn from Lake Houston to simulate withdrawals for the NEWPP plant expansion, as this is the estimated additional withdrawal once NEWPP is at full capacity.

The time from 2009 to 2017 spanned an extreme range of climatological and hydrological variability. The years 2009 and 2010 were average in terms of meteorological patterns, based on the Global Summary of the Year from 2000 to 2018 for George Bush Intercontinental Airport (<https://gis.ncdc.noaa.gov/maps/ncei/cdo/annual>). In 2011, most of Texas, including Lake Houston and all its tributary watersheds, experienced one

of the driest years in modern Texas history (Winters 2013). After the 2011 drought ended, the meteorological patterns for the Lake Houston region have either been normal to extremely wet except for another dry period in 2013. For the years 2015, 2016, and 2017, there was at least one extreme precipitation event each year, culminating in Hurricane Harvey at the end of August 2017.

The first two scenarios included a sustained diversion of LBIT flow: Scenario 1 included 240 MGD (737 ac-ft) for the entire period and Scenario 2 included 320 MGD (982 ac-ft) for the entire period. Scenario 1 results in a net deficit of 80 MGD (246 ac-ft) being added to Lake Houston, as LBIT flow is 240 MGD versus 320 MGD for the additional NEWPP withdrawal. For Scenario 2, LBIT flow and NEWPP diversions are balanced at 320 MGD each. The final scenario, Scenario 2A, was set up like Scenario 2 except during the long drought period of late 2010 through 2011, an extra 80 MGD

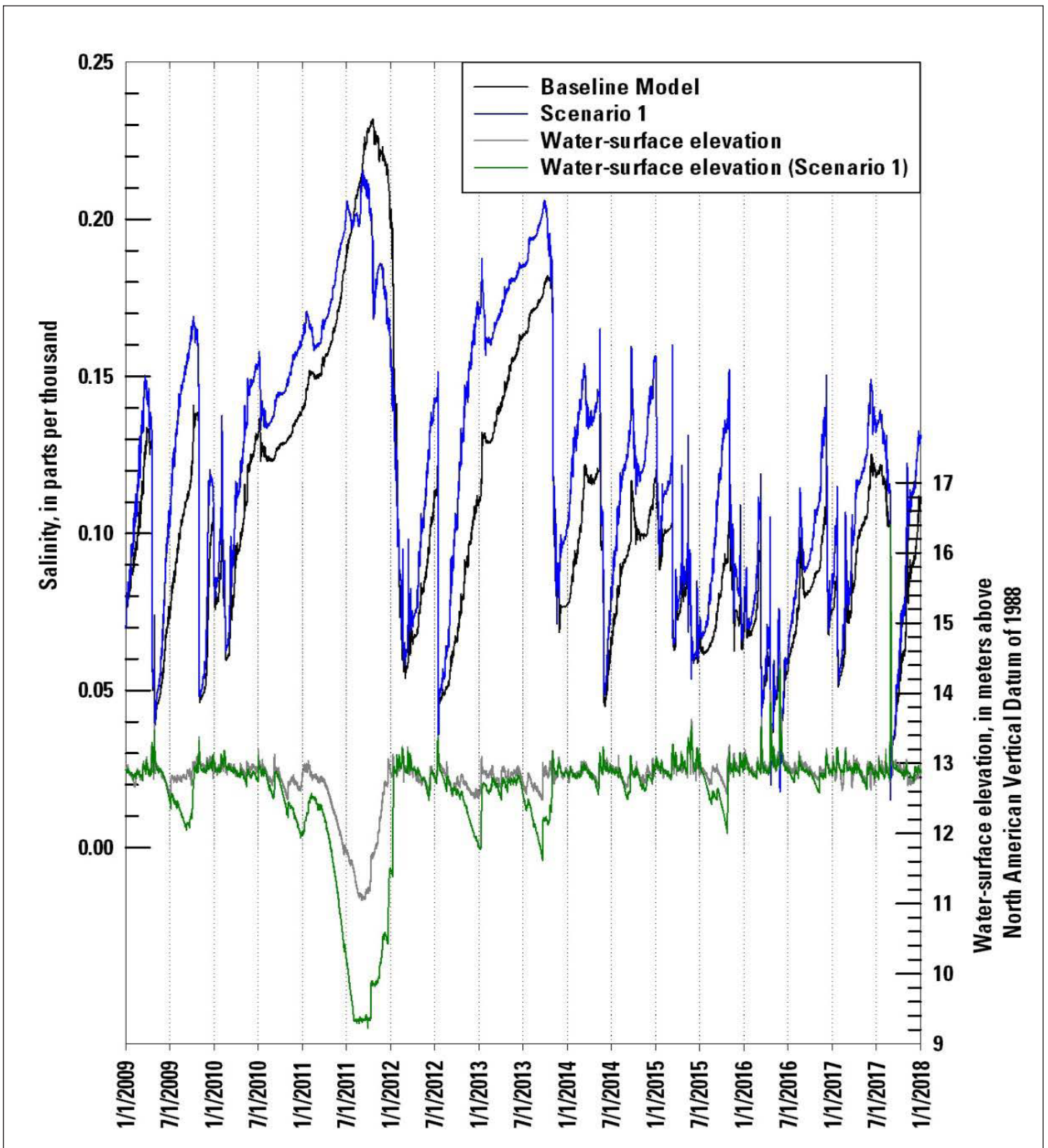


Figure 7. Scenario 1 simulated salinity (in parts per thousand) for Lake Houston at mouth of Jack’s Ditch near Houston, Texas (USGS 295554095093401) at 1.8-meters (5.9-feet) depth, 2009–2017. Also shown is the baseline (calibrated and verified) model simulated salinity at the same location, measured Lake Houston water-surface elevation, and the simulated Lake Houston water-surface elevation for Scenario 1.

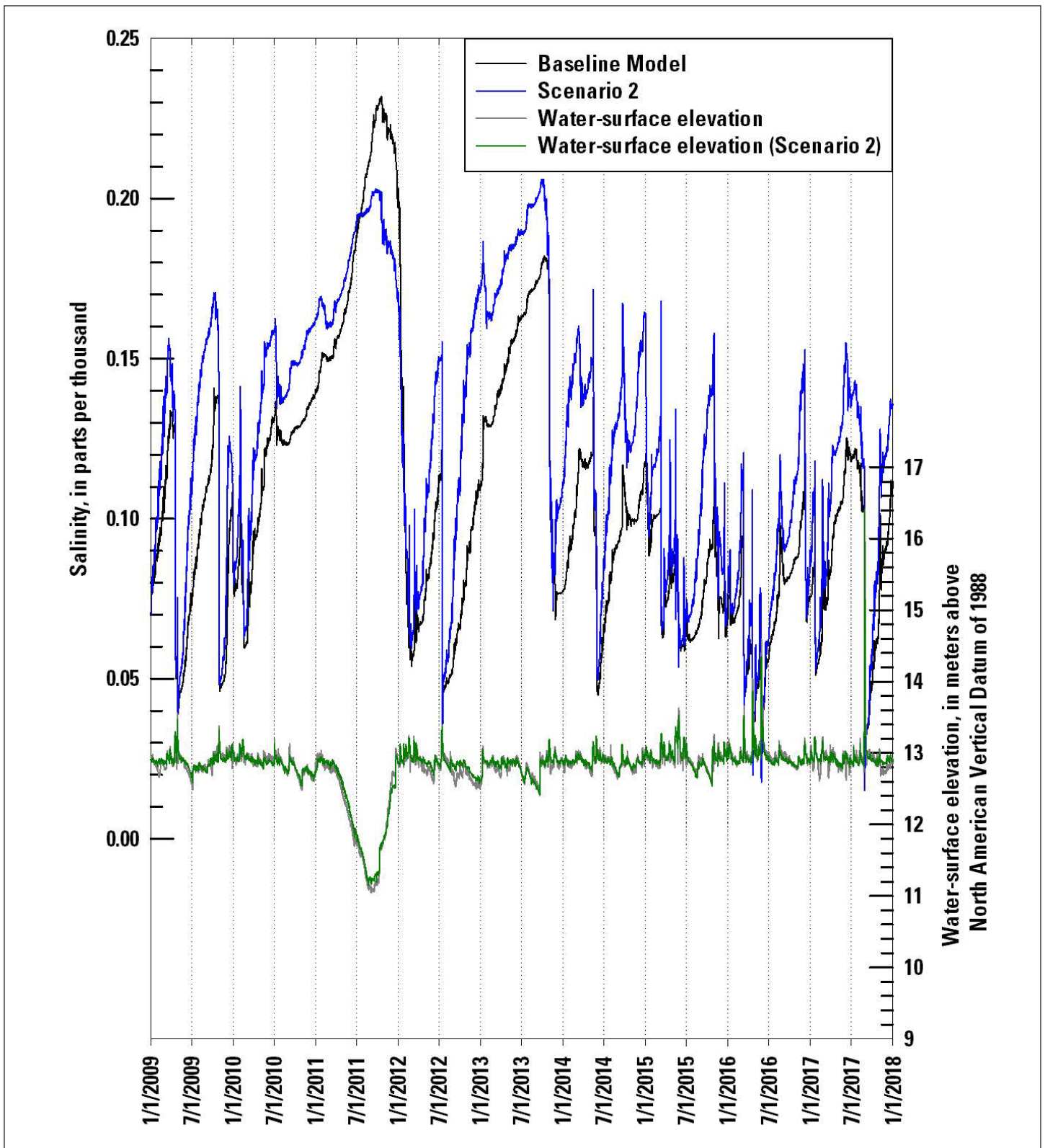


Figure 8. Scenario 2 simulated salinity (in parts per thousand) for Lake Houston at mouth of Jack's Ditch near Houston, Texas (USGS 295554095093401) at 1.8-meters (5.9-feet) depth, 2009–2017. Also shown is the baseline (calibrated and verified) model simulated salinity at the same location, measured Lake Houston water-surface elevation, and the simulated Lake Houston water-surface elevation for Scenario 2.

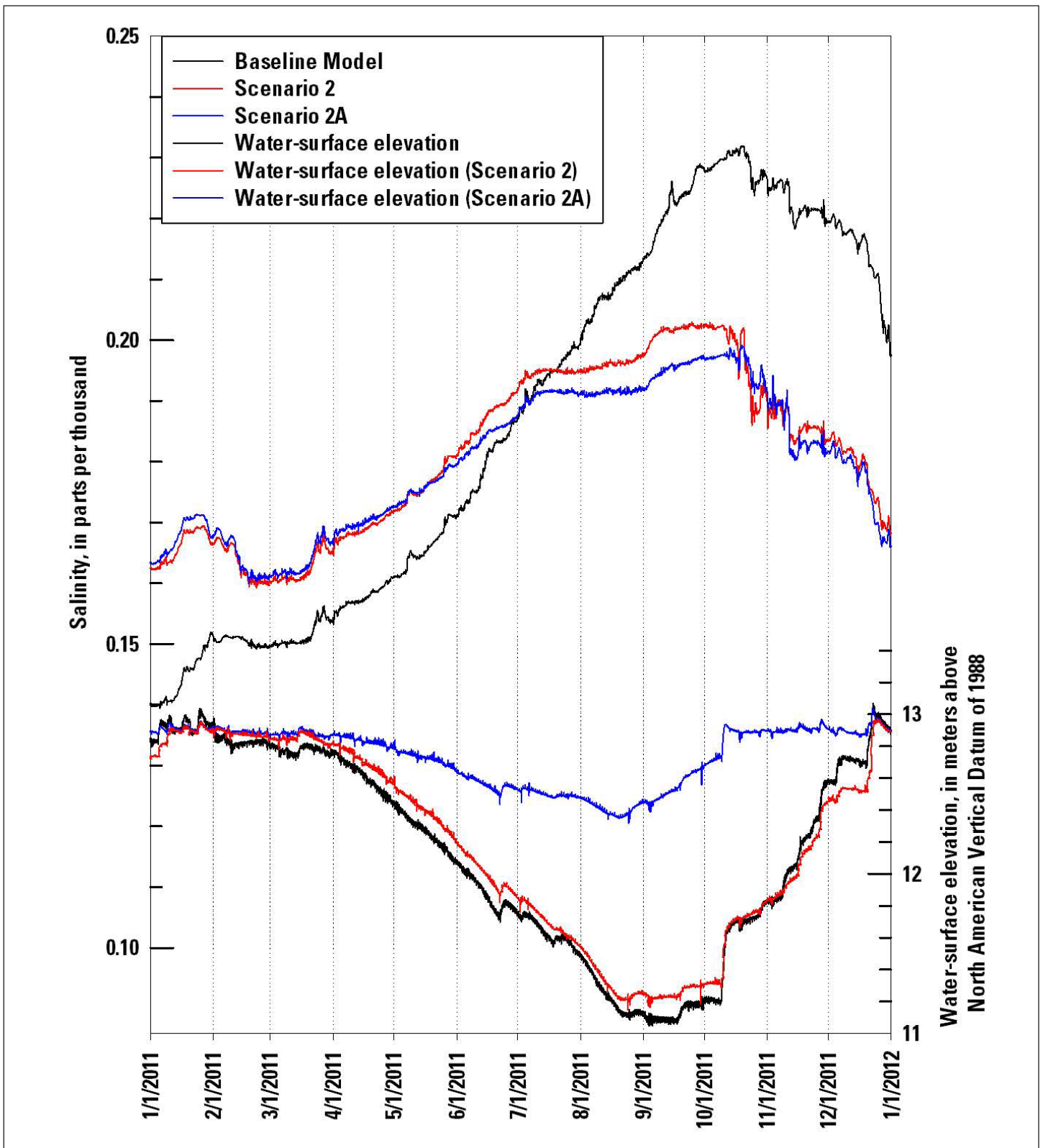


Figure 9. Scenarios 2 and 2A simulated salinity (in parts per thousand) for Lake Houston at mouth of Jack’s Ditch near Houston, Texas (USGS 295554095093401) at 1.8-meters (5.9-feet) depth, 2011. Also shown is the baseline (calibrated and verified) model simulated salinity at the same location, measured Lake Houston water-surface elevation, and the simulated Lake Houston water-surface elevation for Scenarios 2 and 2A.

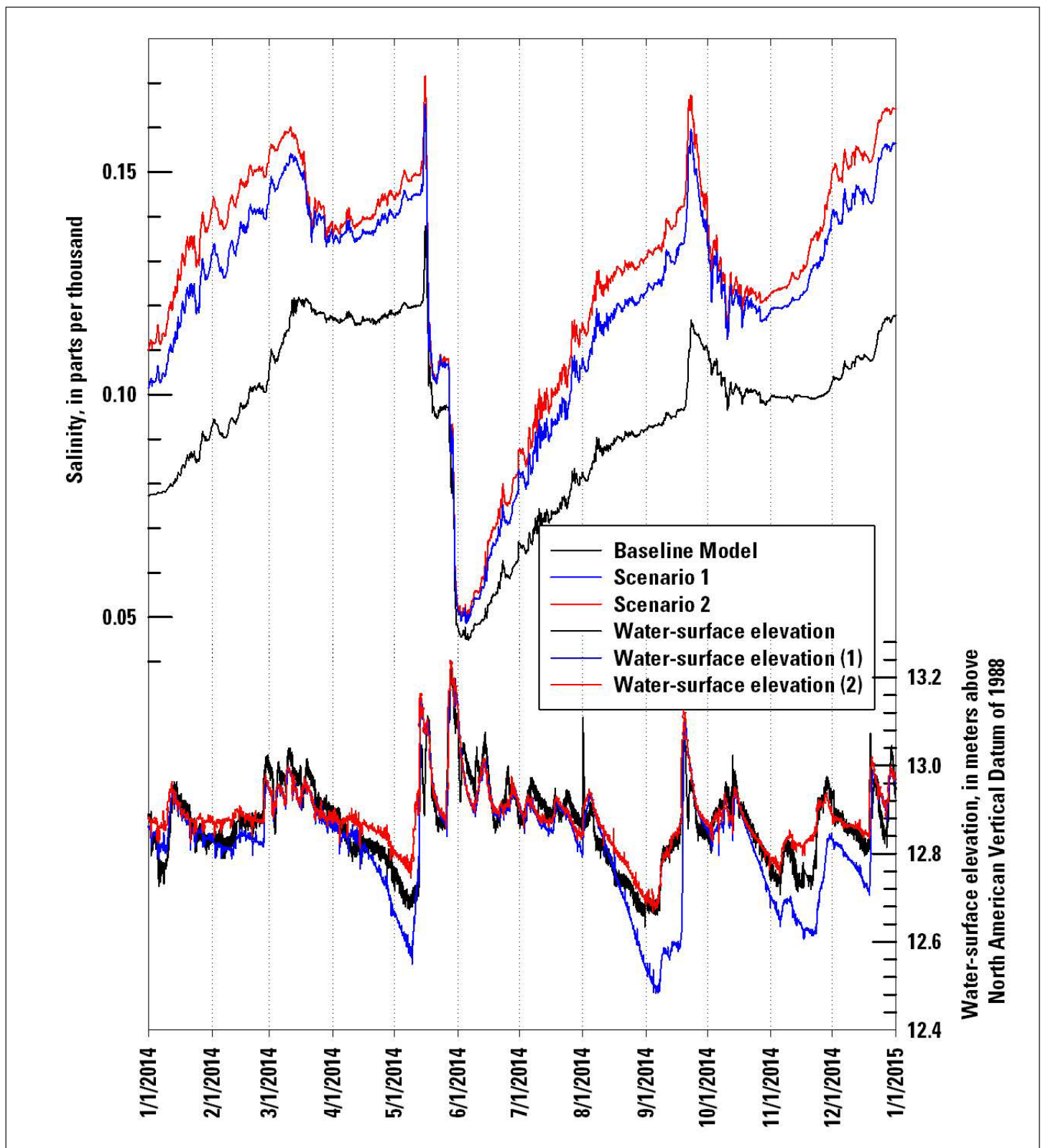


Figure 10. Scenarios 1 and 2 simulated salinity (in parts per thousand) for Lake Houston at mouth of Jack's Ditch near Houston, Texas (USGS 295554095093401) at 1.8-meters (5.9-feet) depth, 2014. Also shown is the baseline (calibrated and verified) model simulated salinity at the same location, measured Lake Houston water-surface elevation, and the simulated Lake Houston water-surface elevation for Scenarios 1 and 2.

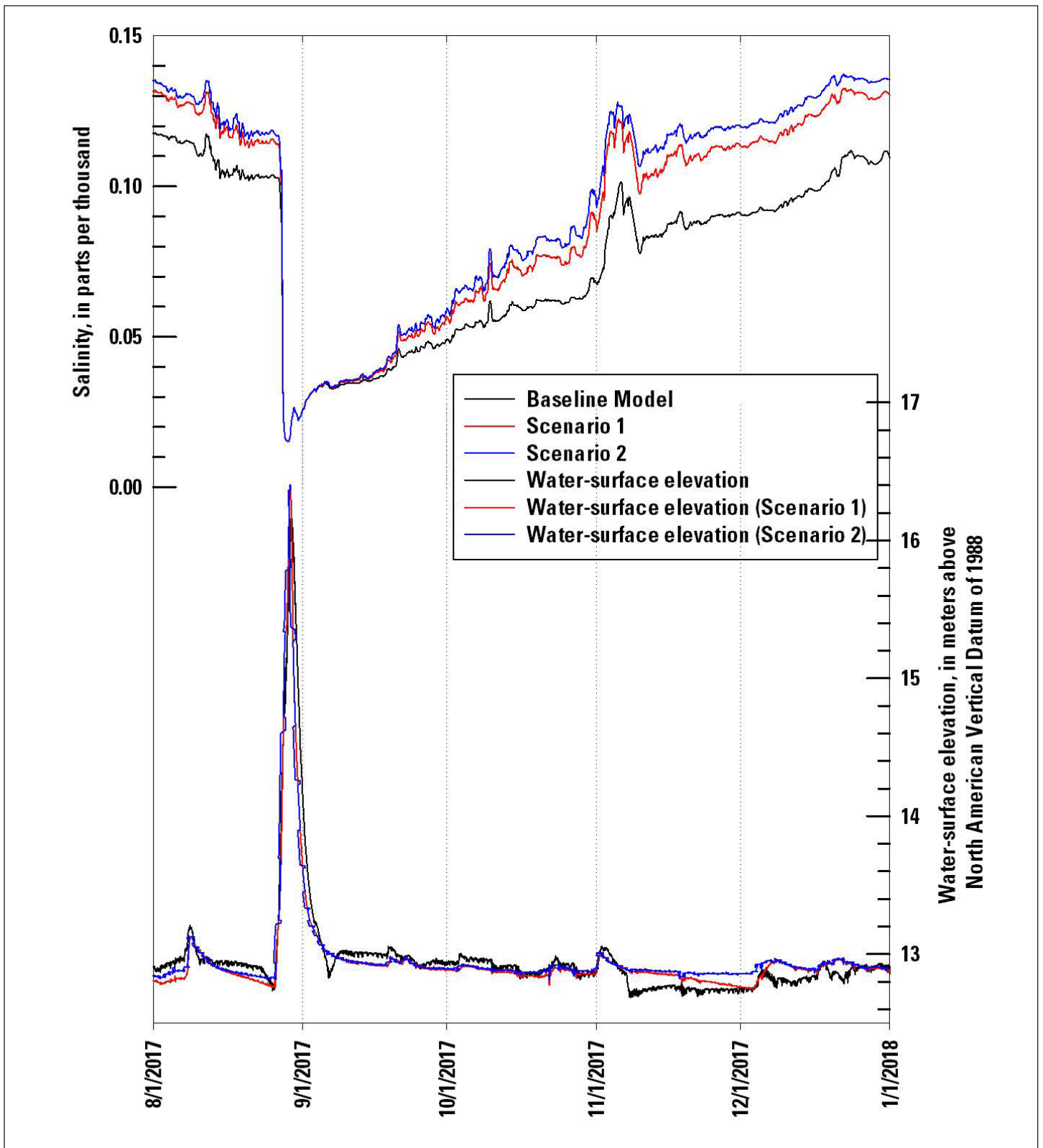


Figure 11. Scenarios 1 and 2 simulated salinity (in parts per thousand) for Lake Houston at mouth of Jack’s Ditch near Houston, Texas (USGS 295554095093401) at 1.8-meters (5.9-feet) depth, 2017. Also shown is the baseline (calibrated and verified) model simulated salinity at the same location, measured Lake Houston water-surface elevation, and the simulated Lake Houston water-surface elevation for Scenarios 1 and 2.

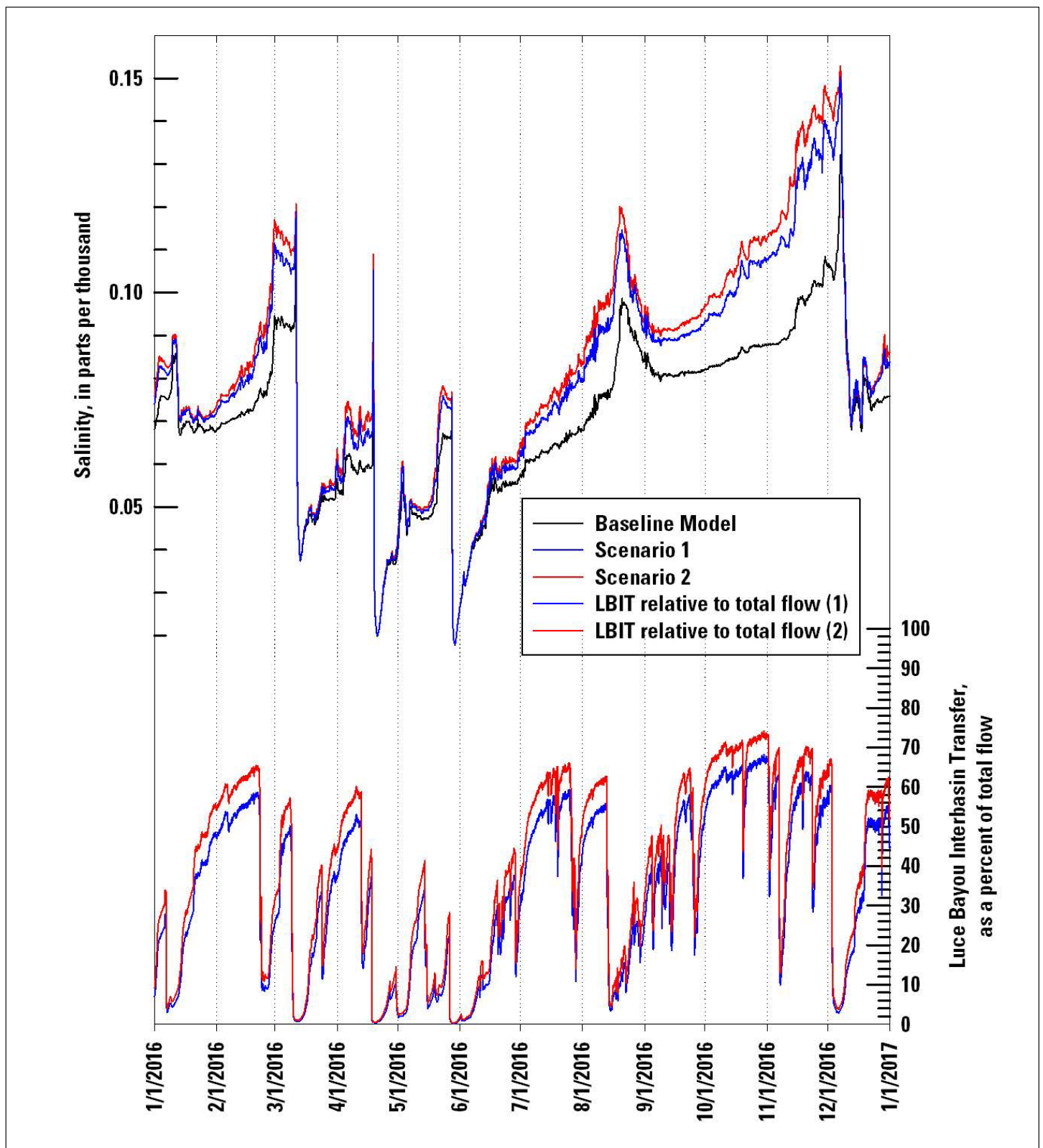


Figure 12. Luce Bayou Interbasin Transfer flow, as a percent of the cumulative flow from the Luce Bayou Interbasin Transfer and the seven tributaries, 2016. Also shown is the baseline (calibrated) model simulated salinity for Lake Houston at mouth of Jack's Ditch near Houston, Texas (USGS 295554095093401) at 1.8-meters (5.9-feet) depth for 2016, and the simulated salinities for Scenarios 1 and 2.

of LBIT flow was diverted from the Trinity River for a total of 400 MGD (1,228 ac-ft).

Scenario 1 was run from October 3, 2008, through December 31, 2017 (Figure 7). Model conditions remained identical to the baseline model (calibrated/verified model), except for a sustained LBIT flow of 240 MGD and NEWPP withdrawal of 320 MGD from January 1, 2009, through December 31, 2017. Prior to January 1, 2009, the model was run for the last 3 months of 2008 as a model warm-up period to avoid a start-up bias. The most striking difference for Scenario 1 from the baseline model was the larger drop in the water-surface elevation, particularly during the drought year of 2011. Smaller drops occurred again in 2012, 2013, and 2015. These drops were the net effect of an increase of 80 MGD in withdrawals over the LBIT flow. The effect on salinity was not the same for each of these 4 years with water deficits compared to the baseline model. In 2011, the water deficit caused water-surface elevations to drop approximately 2 m (6.6 ft) more than the baseline model, but the salinity for Scenario 1 rose less than the baseline model. For the other years with water deficits, the salinity was generally higher for Scenario 1 than the baseline model.

Scenario 2 had the same model conditions as Scenario 1, except the LBIT flow was set to 320 MGD rather than 240 MGD (Figure 8). Scenario 2 showed similar trends to Scenario 1, except the peak salinity in 2011 was more buffered by LBIT flow for Scenario 2. For the subsequent years with water deficits (2012, 2013, and 2015) in Scenario 2, the high salinity values for those years were slightly more pronounced for Scenario 2 than Scenario 1 although these differences were subtle. Peak salinity values for Scenario 2 were approximately 0.01 ppt higher than Scenario 1—for example, the salinity peaks in 2014 were 0.17 ppt in Scenario 2 as opposed to 0.16 ppt in Scenario 1. Water-surface elevations in Scenario 2 were almost the same as the baseline model, as the water deficits caused by the increased NEWPP withdrawals were canceled out by increased LBIT flow.

Scenario 2A had the same model conditions as Scenario 2, except the LBIT flow was set to 400 MGD rather than 320 MGD (Figure 9) during the prolonged 2011 drought; LBIT flow was 400 MGD from November 1, 2010, through December 31, 2011. This scenario was designed to simulate the conditions of sustained 320 MGD LBIT flow with an extra 80 MGD of supplemental LBIT flow during the severe drought when reservoir levels dropped by almost 2 m (6.6 ft). This scenario also assumes that LBIT flow could be used during a drought, because it is likely the Trinity River would also be under similar drought conditions. With the additional 80 MGD for all of 2011, the water-surface elevations only dropped by 0.5 m (1.6 ft) as opposed to the 2 m (6.6 ft) for both the baseline model and Scenario 2. Salinity for Scenario 2A is similar to Scenario 2, where the salinity is buffered by almost 0.04 ppt.

DISCUSSION

These long-term scenarios were intended to help understand the long-term effects of sustained pumping of Trinity River water through the LBIT to Lake Houston. Because the Trinity River has elevated specific conductance compared to the Lake Houston tributaries, these scenarios were designed to help understand the relative increases or decreases in specific conductance that could occur because of the LBIT. Using salinity as a proxy for elevated specific conductance and total dissolved solids, elevated salinity requires additional water treatment efforts and thereby would result in an increase in water treatment costs ([EWT Water Technology 2018](#)). Alternatively, if salinity does not increase or goes down during certain periods, the risk to elevated water treatment costs goes down. It is important to note that salinity is not completely analogous to specific conductance or total dissolved solids ([Atekwana et al. 2004](#); [Fondreist 2014](#)). Nonetheless, salinity was the best surrogate parameter available for analysis as a sub-module within the Lake Houston EFDC model.

Overall, hydrological and climatological forcing had the largest effect on salinity in Lake Houston. Although Lake Houston salinities for the LBIT scenarios were higher than the baseline for most of the modeled time (2009–2017), the highest salinities were attributed to climatological forcing (i.e., warm, dry periods) rather than introducing LBIT flow. For example, the highest salinity levels during the entire 2009–2017 period were the salinity values in 2011 (Figure 6; Figure 9). Long periods of evapotranspiration concentrated the dissolved constituents within Lake Houston. As the water-surface elevation dropped without freshwater replenishing Lake Houston, such as during 2011 and to a lesser degree during dry periods in other years such as 2012 through 2015, the salinity would increase. In 2014, the measured salinity (Figure 10) steadily rose to 0.15 ppt in May and then quickly dropped due to a series of large inflow events from the tributaries. Salinity then steadily rose again to 0.11 ppt by the end of the 2014 after bottoming out at 0.05 ppt. In contrast, the Hurricane Harvey effect can clearly be seen in late August and early September 2017 (Figure 11). Water-surface elevations rose by approximately 3.5 m (11.5 ft) to nearly 16.5 m (54.1 ft), whereas measured salinity dropped to 0.02 ppt. This forcing event equalized LBIT Scenarios 1 and 2 to the same as the measured salinity—both events had elevated salinity before the event. This effect of equalized salinity lasted for over a month past the end of Hurricane Harvey.

Hydrological and climatological forcing had a strong effect on salinity over shorter periods, but the simulated LBIT flow did have a long-term effect on Lake Houston water. As the Trinity River water generally had higher salinity than the tributary inflows into Lake Houston, the simulated scenarios indicated that this water would cause Lake Houston's salinity to increase during much of the simulated period. This relative increase in

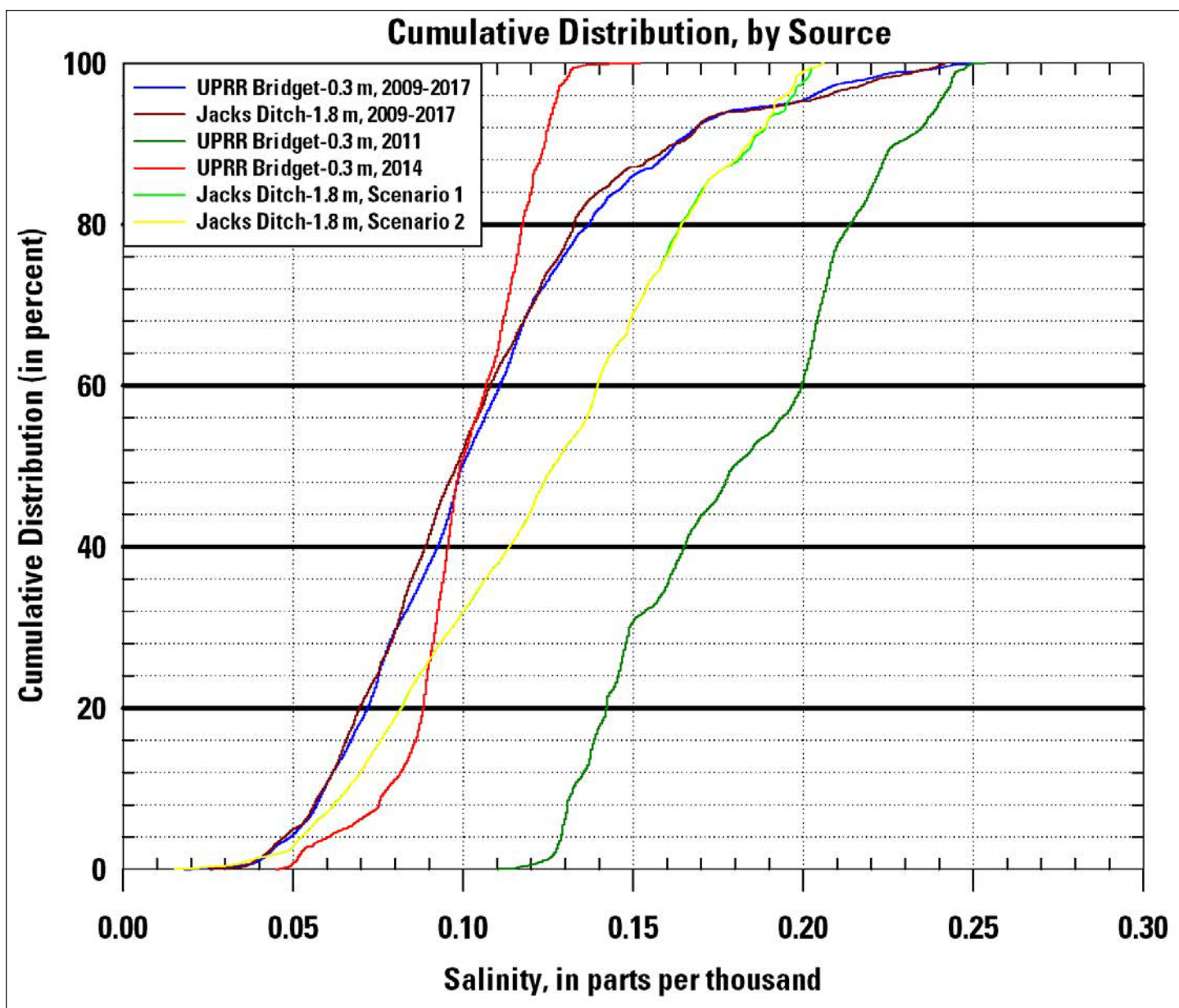


Figure 13. Cumulative distribution, by source, of the salinity (in parts per thousand) for the following measured data: UPRR Bridge at 0.3-meter (1-foot) depth (2009–2017), UPRR Bridge at 0.3-meter (1-foot) depth (2011), UPRR Bridge at 0.3-meter (1-foot) depth (2014), and Jack’s Ditch at 1.8-meters (5.9-feet) depth (2009–2017). Also shown is Jack’s Ditch at 1.8-meters (5.9-feet) depth (2009–2017) for Scenario 1 and Scenario 2.

salinity from LBIT flow can be seen across a wide spectrum of the 2009–2017 period. Scenario 1 (Figure 7) and Scenario 2 (Figure 8) both show elevated salinity over the measured salinity for most of the 9-year period. The LBIT effect in Scenarios 1 and 2 could also be large, often greater than 0.05–0.06 ppt (Figure 10). While increased salinities (i.e., increased total dissolved solids) could potentially increase treatment costs, the LBIT scenarios did not introduce salinities beyond the natural variation observed from 2009 to 2017. Therefore, the necessity for increased treatment capacity due to substantial changes in total dissolved solids from LBIT flow would be unlikely.

The effect of the LBIT flow on salinity can also be shown through the ratio of LBIT flow to the cumulative sum of LBIT flow and the seven tributaries for Scenario 1 (240 MGD) and Scenario 2 (320 MGD; Figure 12). In 2016, simulated periods with low LBIT flow relative to the overall flow, such as late April and early May 2016, had a lower salinity. Alternatively, simulated periods with mostly high LBIT ratios, such as the periods starting in July 2016 and later in October 2016, had larger deviations for both scenarios from the baseline model (Figure 12). In October and November, the LBIT flow was up 68% and 74% of the entire inflow into Lake Houston for

Scenarios 1 and 2, respectively—this period also had the higher salinities and the largest deviations between the baseline model and the two LBIT scenarios.

Another way to understand the effects of both hydrological/climatological forcing and LBIT flow on Lake Houston salinity is to look at measured (or simulated) salinity (in ppt) as cumulative distributions (Figure 13). This shows the percent of measurements for the different locations or scenarios that are at or below a salinity value. For example, the 2011 measured data for the UPRR Bridge at 0.3 m (1 ft) depth was at or below 0.20 ppt for 60% of the measurements. In contrast, 40% of the measurements for this location were above 0.20 ppt in 2011. This year was isolated from the 2009–2017 cumulative measured results, shown with the UPRR Bridge at 0.3 m (1 ft) and Jack's Ditch at 1.8 m (5.9 ft), to show the much higher salinities throughout 2011. Alternatively, almost all measured salinities in 2014 for the UPRR Bridge at 0.3 m (1 ft) were below 0.12 ppt. The cumulative results show a wide distribution of salinities, with only about 5% of the values exceeding 0.20 ppt. These two cumulative curves for the two different locations also show there is not a large difference between these two measured locations, despite differences in depth and location.

For Scenario 1 and Scenario 2, the cumulative distributions were almost identical between the two scenarios. When viewed over time, these two scenarios did have subtle differences across the 9-year period (Figure 7; Figure 8), but clearly these differences were small when shown as cumulative distributions. Both scenarios also had higher salinities over more time compared to the measured cumulative distributions (2009–2017; Figure 13), so the LBIT did cause elevated Lake Houston salinities over most of the modeled time. However, the highest values were in the measured data and baseline scenario. The two LBIT scenarios did not go above 0.21 ppt whereas the baseline scenario was above 0.21 ppt approximately 5% of the time at Jack's Ditch (Figure 13).

Another conclusion from the LBIT flow scenarios was the simulated effect of LBIT flow on water-surface elevations. Scenario 2A was meant to help understand whether LBIT flow could be used to augment water-surface elevations during periods of drought or prolonged dry periods. Based on Figure 9, the water-surface elevation only dropped to 12.4 m (40.7 ft) for Scenario 2A as opposed to close to 11 m (36.1 ft) for both the measured water-surface elevations and Scenario 2. Scenario 2A added an extra 80 MGD for over a year, a substantial amount of additional flow. Less flow could have been added to the 320 MGD for Scenario 2, and the water-surface elevation drop would have increased but still not have been as much as during the actual 2011 drought. This shows that LBIT flow could be used during a drought, assuming Trinity River flows would support pulling an additional amount of water. Until

more modeling has been done with the Trinity River, such as utilizing a linked reservoir operations management model similar to the upper Brazos River framework (Zhao et al. 2016), it remains to be determined the maximum amount of overall LBIT flow from the Trinity River that could occur during a drought such as 2011.

SUMMARY

The USGS, in cooperation with Exxon Mobil Corporation, updated the original Lake Houston EFDC model (Rendon and Lee 2015) for predicting water-surface elevation, residence time, water temperature, and salinity. With modifications to the original Lake Houston EFDC model, the potential effects of the upcoming LBITP on water-surface elevations and salinity in Lake Houston were evaluated using three hypothetical scenarios. The modeling scenarios focused on the long-term effects of sustained pumping of Trinity River water through the LBIT to Lake Houston.

Overall, the long-term flow simulations indicated that the LBIT would affect salinity in Lake Houston. During very dry periods, the LBIT flow acted as a buffer on Lake Houston, limiting maximum salinity. Otherwise, the LBIT flow generally caused the salinity of Lake Houston to increase over the measured data that did not include LBIT flow. While increased salinities (i.e., increased total dissolved solids) could potentially increase treatment costs, the LBIT scenarios did not introduce salinities beyond the natural variation observed from 2009 to 2017.

Hydrological and climatological forcing has the largest effect on salinity in Lake Houston, at least in terms of the extreme salinity values. The highest salinity levels during the entire 2009–2017 period was in 2011. Long periods of evapotranspiration concentrated the dissolved constituents within Lake Houston. As the water-surface elevation dropped without freshwater replenishing Lake Houston, the salinity would rise substantially. Also, large inflow events caused by large storms or hurricanes cause very low salinity and would equalize the effects of the LBIT flow because the LBIT flux would be overwhelmed by tributary inflows and runoff.

LBIT flow could also be used to supplement water levels during extreme droughts. This study found that an extra 80 MGD above a balanced 320-MGD LBIT flow would substantially diminish water-level elevation drops during a 2011-type drought event. However, this scenario would need further evaluation using a linked reservoir operations management model for the entire linked system, because this would affect the water management plan for the entire region, including Lake Houston, Lake Livingston, and the lower Trinity River.

ACKNOWLEDGMENTS

Funding for this study was provided by ExxonMobil. This article presents a compilation of information supplied mainly from the USGS, the City of Houston, the CWA, and the San Jacinto River Authority. Special thanks to Greg Olinger and Jordan Austin for compiling daily water withdrawal records from Lake Houston dating back to 2009. The authors thank reviewers for helpful comments and suggestions for improving the original manuscript. Any use of trade, firm, or product names is for descriptive purposes only and does not imply endorsement by the U.S. Government.

REFERENCES

- [AECOM] AECOM Technical Services, Inc. 2011. Preliminary engineering report for Luce Bayou Interbasin Transfer Project. Los Angeles (California): AECOM Technical Services, Inc. 272 p. Prepared for Coastal Water Authority. Available from: <https://www.coastalwaterauthority.org/files/contractoroutreach/lucebayouproject/documents/PER-VOL1-01282011.pdf>.
- Atekwana EA, Rowe RS, Werkema DD Jr, Legall FD. 2004. The relationship of total dissolved solids measurements to bulk electrical conductivity in an aquifer contaminated with hydrocarbon. *Journal of Applied Geophysics*. 56(4):281-294. Available from: <https://doi.org/10.1016/j.jappgeo.2004.08.003>.
- Bawden GW, Johnson MR, Kasmarek MC, Brandt J, Middleton CS. 2012. Investigation of land subsidence in the Houston-Galveston region of Texas by using the Global Positioning System and interferometric synthetic aperture radar, 1993–2000. Reston (Virginia): U.S. Geological Survey. 98 p. Scientific Investigations Report 2012-5211. Available from: <https://pubs.usgs.gov/sir/2012/5211/pdf/sir2012-5211.pdf>.
- Beussink AM, Burnich MR. 2009. Continuous and discrete water-quality data collected at five sites on Lake Houston near Houston, Texas, 2006–08. Reston (Virginia): U.S. Geological Survey. 30 p. Data Series 485. Available from <https://pubs.usgs.gov/ds/485/pdf/ds485.pdf>.
- Brashier V. 2011 Aug 16. Pictures tell the story: Drought draining Lake Houston, leading to mandatory conservation order. *Houston Chronicle*. Available from: <https://www.chron.com/neighborhood/article/Pictures-tell-the-story-Drought-draining-Lake-9421465.php>.
- Chow VT, Maidment DR, Mays LW. 1988. *Applied hydrology*. New York (New York): McGraw-Hill Book Co. 572 p.
- [COH DWO] City of Houston Drinking Water Operations. 2006. City of Houston surface water supply sources. Available from: https://www.publicworks.houstontx.gov/sites/default/files/assets/003-regional_water_supply_map.pdf.
- [COH DWO] City of Houston Drinking Water Operations. n.d. Drinking water operations. Available from: <https://www.publicworks.houstontx.gov/pud/drinkingwater.html>.
- Combs S. 2012. The impact of the 2011 drought and beyond. Austin (Texas): Texas Comptroller of Public Accounts. 16 p. Available from: https://texashistory.unt.edu/ark:/67531/metaph542095/m2/1/high_res_d/txcs-0790.pdf.
- Craig PM. 2017. User's manual for EFDC_Explorer 8.3: A pre/post processor for the Environmental Fluid Dynamics Code. Edmonds (Washington): DSI, LLC. 454 p.
- [CWA] Coastal Water Authority. 2019. Coastal Water Authority: Minutes of regular meeting, February 13, 2019. Available from: https://www.coastalwaterauthority.org/files/meetingnotices/publicminutes/Feb_13_2019_Meeting_Minutes.pdf.
- [CWA] Coastal Water Authority. n.d. What is the Luce Bayou Interbasin Transfer Project? Available from: <https://www.coastalwaterauthority.org/contractor-outreach/luce-bayou-project/about-cwa/what-is-the-luce-bayou-interbasin-transfer-project>.
- Dynamic Solutions. 2013. Lake Thunderbird report for nutrient, turbidity, and dissolved oxygen TMDLs. Oklahoma City (Oklahoma): Oklahoma Department of Environmental Quality. 306 p. Prepared for Oklahoma Department of Environmental Quality. Available from: https://www.epa.gov/sites/production/files/2015-10/documents/lakethunderbird_ok.pdf.
- Elçi S, Work PA, Hayter EJ. 2007. Influence of stratification and shoreline erosion on reservoir sedimentation patterns. *Journal of Hydraulic Engineering*. 133(3):255-266. Available from: [https://doi.org/10.1061/\(ASCE\)0733-9429\(2007\)133:3\(255\)](https://doi.org/10.1061/(ASCE)0733-9429(2007)133:3(255)).
- Eltagouri M. 2016 May 19. Chicago losing population, could be overtaken by Houston as 3rd-largest. *Chicago Tribune*. Available from: <https://www.chicagotribune.com/news/breaking/ct-census-chicago-losing-population-met-20160518-story.html>.
- ESRI. 2018. ArcGIS Desktop 10. Redlands (California): Environmental Systems Research Institute.
- EWT Water Technology. 2018. Demineralized water in boiler feed water treatment applications: comparison between ion exchange and membrane separation processes. Available from: <http://www.ewt-wasser.de/en/knowledge/demineralised-water.html>.

- [Fondreist] Fondreist Environmental Learning Center. 2014. Conductivity, salinity, and total dissolved solids. Available from: <https://www.fondreist.com/environmental-measurements/parameters/water-quality/conductivity-salinity-tds/>.
- Gabrysch RK. 1982. Ground-water withdrawals and land-surface subsidence in the Houston-Galveston region, Texas, 1906–80. Austin (Texas): U.S. Geological Survey. 74 p. Open File Report 82-571. Available from: <https://pubs.usgs.gov/of/1982/0571/report.pdf>.
- Hamrick JM. 1992. A three-dimensional Environmental Fluid Dynamics Computer Code: Theoretical and computational aspects. Gloucester Point (Virginia): Virginia Institute of Marine Science. 65 p. Special Report No. 317. Available from: <http://publish.wm.edu/cgi/viewcontent.cgi?article=1713&context=reports>.
- Hamrick JM. 1996. User's manual for the Environmental Fluid Dynamics Computer Code. Gloucester Point (Virginia): Virginia Institute of Marine Science. 224 p. Special Report No. 331. Available from: <https://publish.wm.edu/cgi/viewcontent.cgi?article=2043&context=reports>.
- Helsel DR, Hirsch RM. 2002. Statistical methods in water resources. Reston (Virginia): U.S. Geological Survey. 524 p. Techniques of Water-Resources Investigations 4-A3. Available from: <https://pubs.usgs.gov/twri/twri4a3/twri4a3.pdf>.
- [HGSD] Harris-Galveston Subsidence District. 2020. About the District. Available from: <https://hgsubsidence.org/about/>.
- Ji ZG, Morton MR, Hamrick JM. 2004. Modeling hydrodynamic and water quality processes in a reservoir. In: Spaulding ML, editor. Estuarine and Coastal Modeling. Monterey (California): American Society of Civil Engineers. p. 608-627. Available from: [https://doi.org/10.1061/40734\(145\)38](https://doi.org/10.1061/40734(145)38).
- Ji ZG. 2017. Hydrodynamics and water quality: Modeling rivers, lakes, and estuaries. 2nd edition. Hoboken (New Jersey): John Wiley and Sons. 612 p.
- Jin KR, Ji ZG, James RT. 2007. Three-dimensional water quality and SAV modeling of a large shallow lake. Journal of Great Lakes Research. 33(1):28-45. Available from: [https://doi.org/10.3394/0380-1330\(2007\)33\[28:T WQASM\]2.0.CO;2](https://doi.org/10.3394/0380-1330(2007)33[28:T WQASM]2.0.CO;2).
- Kasmarek MC, Johnson MR. 2013. Groundwater withdrawals 1976, 1990, and 2000–10 and land-surface-elevation changes 2000–10 in Harris, Galveston, Fort Bend, Montgomery, and Brazoria Counties, Texas. Reston (Virginia): U.S. Geological Survey. 25 p. Scientific Investigations Report 2013-5034. Available from: <https://pubs.usgs.gov/sir/2013/5034/pdf/sir2013-5034.pdf>.
- Legates DR, McCabe GJ Jr. 1999. Evaluating the use of “goodness-of-fit” measures in hydrologic and hydroclimatic model validation. Water Resources Research. 35(1):233-241. Available from: <https://doi.org/10.1029/1998WR900018>.
- Liscum F, Goss RL, Rast W. 1999. Characteristics of water-quality data for Lake Houston, selected tributary inflows to Lake Houston, and the Trinity River near Lake Houston (a potential source of interbasin transfer), August 1983–September 1990. Austin (Texas): U.S. Geological Survey. 62 p. Water-Resources Investigations Report 99-4129. Available from: <https://pubs.usgs.gov/wri/wri99-4129/pdf/wri99-4129.pdf>.
- Liscum F, East JW. 2000. Estimated effects on water quality of Lake Houston from interbasin transfer of water from the Trinity River, Texas. Austin (Texas): U.S. Geological Survey. 55 p. Water-Resources Investigations Report 00-4082. Available from: <https://pubs.usgs.gov/wri/wri00-4082/pdf/wri00-4082.pdf>.
- Miller D, Marks JS. 2018. Coastal Water Authority Luce Bayou Interbasin Transfer project update. Proceedings of the 23rd Annual Conference of the Center for Innovative Grouting Materials and Technology; 2018 March 2; Houston, TX. 2 p. Available from: <http://cigmat.cive.uh.edu/sites/cigmat/files/files/conference/presentation/2018/david-miller.pdf>.
- Mueller DS, Wagner CR, Rehmel MS, Oberg KA, Rainville F. 2013. Measuring discharge with Acoustic Doppler Current Profilers from a moving boat. Reston (Virginia): U.S. Geological Survey. 116 p. Techniques and Methods 3–A22. Available from: <https://pubs.usgs.gov/tm/3a22/>.
- Nash JE, Sutcliffe IV. 1970. River flow forecasting through conceptual models, Part I — A discussion of principles. Journal of Hydrology. 10(3):282-290. Available from: [https://doi.org/10.1016/0022-1694\(70\)90255-6](https://doi.org/10.1016/0022-1694(70)90255-6).
- Rantz SE. 1982. Measurement and computation of streamflow. Washington (District of Columbia): U.S. Geological Survey. 313 p. Water-Supply Paper 2175. Available from: <https://pubs.usgs.gov/wsp/wsp2175/wsp2175.pdf>.
- Rendon SH, Lee MT. 2015. Simulation of the effects of different inflows on hydrologic conditions in Lake Houston with a three-dimensional hydrodynamic model, Houston, Texas, 2009–10. Reston (Virginia): U.S. Geological Survey. 52 p. Scientific Investigations Report 2015-5153. Available from: <https://doi.org/10.3133/sir20155153>.
- Rogers GO, Moore GW, Saginor J, Brody SD. 2012. Impact of lake-level reductions on Lake Conroe area: lake area property values, property tax revenues and sales tax revenue. 54 p. Available from: <https://www.lakeconroe.com/wp-content/uploads/2012/08/Lake-Conroe-Final-Report.pdf>.

- Smith EA. 2019. Lake Houston (Texas) EFDC hydrodynamic model for water-surface elevation and specific conductance simulations, 2009–2017. U.S. Geological Survey data release. Available from: <https://doi.org/10.5066/P9AVUJ73>.
- Sneck-Fahrer D, Milburn MS, East JW, Oden JH. 2005. Water-quality assessment of Lake Houston near Houston, Texas, 2000–2004. Reston (Virginia): U.S. Geological Survey. 64 p. Scientific Investigations Report 2005-5241. Available from: <https://pubs.usgs.gov/sir/2005/5241/pdf/sir2005-5241.pdf>.
- [TWDB] Texas Water Development Board. n.d. Lake Houston (San Jacinto River Basin). Available from: <https://www.twdb.texas.gov/surfacewater/rivers/reservoirs/houston/>.
- [USGS and USDA NRCS] U.S. Geological Survey and U.S. Department of Agriculture, Natural Resources Conservation Service. 2013. Federal Standards and procedures for the National Watershed Boundary Dataset (WBD) (4th ed.). Reston (Virginia): U.S. Geological Survey. 63 p. Techniques and Methods 11–A3. Available from: <https://pubs.usgs.gov/tm/11/a3/>.
- [USGS] USGS Water Data for Texas. 2020. Reston (Virginia): U.S. Geological Survey. Available from: <https://waterdata.usgs.gov/tx/nwis/>.
- Wagner RJ, Boulger RW Jr, Oblinger CJ, Smith BA. 2006. Guidelines and standard procedures for continuous water-quality monitors: station operation, record computation, and data reporting. Reston (Virginia): U.S. Geological Survey. 96 p. Techniques and Methods 1–D3. Available from: <https://pubs.usgs.gov/tm/2006/tm1D3/pdf/TM1D3.pdf>.
- [WHCRWA] West Harris County Regional Water Authority. 2019. WHCRWA/NFBWA surface water supply project. Available from: <https://www.surfacewatersupplyproject.com/>.
- Winters KE. 2013. A historical perspective on precipitation, drought severity, and streamflow in Texas during 1951–56 and 2011. Reston (Virginia): U.S. Geological Survey. 34 p. Scientific Investigations Report 2013–5113. Available from: <https://pubs.usgs.gov/sir/2013/5113/pdf/sir20135113.pdf>.
- Zhao G, Gao H, Naz BS, Kao SC, Voisin N. 2016. Integrating a reservoir regulation scheme into a spatially distributed hydrological model. *Advances in Water Resources*. 98:16–31. Available from: <https://doi.org/10.1016/j.advwatres.2016.10.014>.